DEVELOPMENT OF A COHERENT LIGHT SCANNER

By
W. R. Callen and J. E. Weaver
School of Electrical Engineering

R. G. Shackelford and J. R. Walsh
Engineering Experiment Station

FINAL REPORT
RESEARCH CONTRACT NAS8–28591
9 May 1972 to 8 October 1973

Performed for
NATIONAL AERONAUTICS AND SPACE ADMINISTRATION
George C. Marshall Space Flight Center
Marshall Space Flight Center, Alabama 35812

1973

GEORGIA INSTITUTE OF TECHNOLOGY
Atlanta, Georgia

SCHOOL OF ELECTRICAL ENGINEERING
ENGINEERING EXPERIMENT STATION
Georgia Institute of Technology
Atlanta, Georgia 30332

FINAL REPORT

PROJECT NOS. E-21-618
A-1425

DEVELOPMENT OF A COHERENT LIGHT SCANNER

BY

W. R. Callen, J. E. Weaver, R. G. Shackelford, and J. R. Walsh

RESEARCH CONTRACT NAS8-28591

9 MAY 1972 to 8 OCTOBER 1973

Performed for

NATIONAL AERONAUTICS AND SPACE ADMINISTRATION
George C. Marshall Space Flight Center
Marshall Space Flight Center, Alabama 35812

ABSTRACT

This report describes the construction, operation and testing of a coherent light scanner that was developed and delivered to Marshal Space Flight Center. The scanner incorporates a Coherent Radiation argon laser and light deflecting galvanometer system to deliver a scanned beam perpendicular to a ten cm by ten cm (four inch by four inch) format. The scanner has two basic features that make it particularly suitable for optical processing of data in the form of two dimensional images recorded on film:

1) The scanning beam is random access addressable and is perpendicular to the image plane.

2) The intensity of the scanned beam is controlled such that a constant intensity is maintained after passage through the image plane.

TABLE OF CONTENTS

		Page
I.	INTRODUCTION	1
II.	OPTICAL SYSTEM DESIGN	4
	A. Overall Approach	4
	B. Laser Selection	4
	C. Light Leveling Control System	6
	1. Introduction	6
	2. Simulation of the Feedback Control System	8
	3. Circuit Mechanization	14
	4. Adjustment of the Feedback System	16
	D. Stationary Optics	17
	1. Shutter Design	17
	2. Flat Mirrors	18
	3. Spatial Filter Design	18
	4. Collimating Lens	20
	5. Aperture Assembly	20
	E. Scanning Optics	24
	1. Zoom Lens	25
	2. Parabolic Mirrors	25
	3. Spherical Mirror	31
	4. Figure of Mirrors	33
	5. Galvanometers	33
	F. Interface	33
III.	SYSTEM OPERATION	35
	A. Laser Operation	35
	B. System Alignment	35
	C. Feedback System Adjustments	40
	D. Considerations for Laser Operation at Wavelength Other than 514.5 nm	40
IV.	SYSTEM EVALUATION	41
	A. Measurement of Beam Cross Section	41
	B. Measurement of Scanner Access Time	43
	C. Measurement of the Spatial Invariance of the Fourier Transform of the Scanning Beam	46
V.	ACKNOWLEDGEMENTS	54
APPENDIX A --	SPECIFICATIONS FOR GENERAL SCANNING MODEL 108 PD GALVANOMETERS	55

LIST OF FIGURES

Figure		Page
1.	Basic Optical Processor	2
2.	Laser Scanner Optical System Layout	5
3.	Block Diagram of Light Leveling Control System	7
4.	Block Diagram of Feedback Control System to be Simulated with MIMIC	9
5.	MIMIC Program Listing	11
6.	Schematic Diagram of Preamplifier	15
7.	Shutter Arm and Cavity Detail	19
8.	Scaling of Aerial Photograph	22
9.	Spot Size Spreading	23
10.	Format Projection on Parabolic Mirror Surface	27
11.	Deviation of Parabola from a Circle	28
12.	Deviation of Parabolic Mirror from a Sphere	30
13.	Spherical Mirror Diameter Determination	32
14.	Spherical Mirror Focal Length Considerations	34
15.	Detail of Beam Profile Measuring Device	42
16.	1.8 mm Diameter Aperture Beam Profile	44
17.	2.7 mm Diameter Aperture Beam Profile	45
18.	Galvanometer Response Time Test Layout	47
19.	Galvanometer Response	48
20.	Fourier Transform Spatial Invariance Test Layout	49
21.	Photomicrographs of Fourier Transform Patterns	51
22.	Scanner During Operational Test at Georgia Tech	53

I. INTRODUCTION

For experiments involving the processing of large amounts of data stored as a two-dimensional scene, such as on film, optical techniques provide the most convenient methods. Using these techniques, one can perform complicated mathematical operations, such as two-dimensional Fourier transforms and correlation functions, almost instantaneously. Optical methods are particularly useful for pattern recognition when the presence or absence of certain features in the data are to be determined.

A schematic diagram of an optical processing system is shown in Figure 1. An image is placed in the input plane either in the form of film or by an image forming light modulator. The spatial Fourier transform of the input image appears in the transform plane. In this plane is placed a matched filter such as a computer generated binary hologram. The degree of correlation of the input image with the matched filter in the transform plane is indicated by the intensity of a spot of light in the retransform plane. If the input image is not centered on the optical axis, the spot in the correlation plane shifts by a distance proportional to the misregistration distance.

For certain applications, it is desirable to optically address small areas of the image plane without illuminating the entire surface. In addition, spatial invariance of the optical Fourier transform operation requires that the incident beam remain parallel to the optical axis (perpendicular to the film plane) during the scanning of these small areas. Thus, to optically process selected areas of the film plane, a parallel beam scanner must be developed.

One of the difficulties in ascertaining the amount of correlation of one image compared to another is that the absolute intensity of the correlation

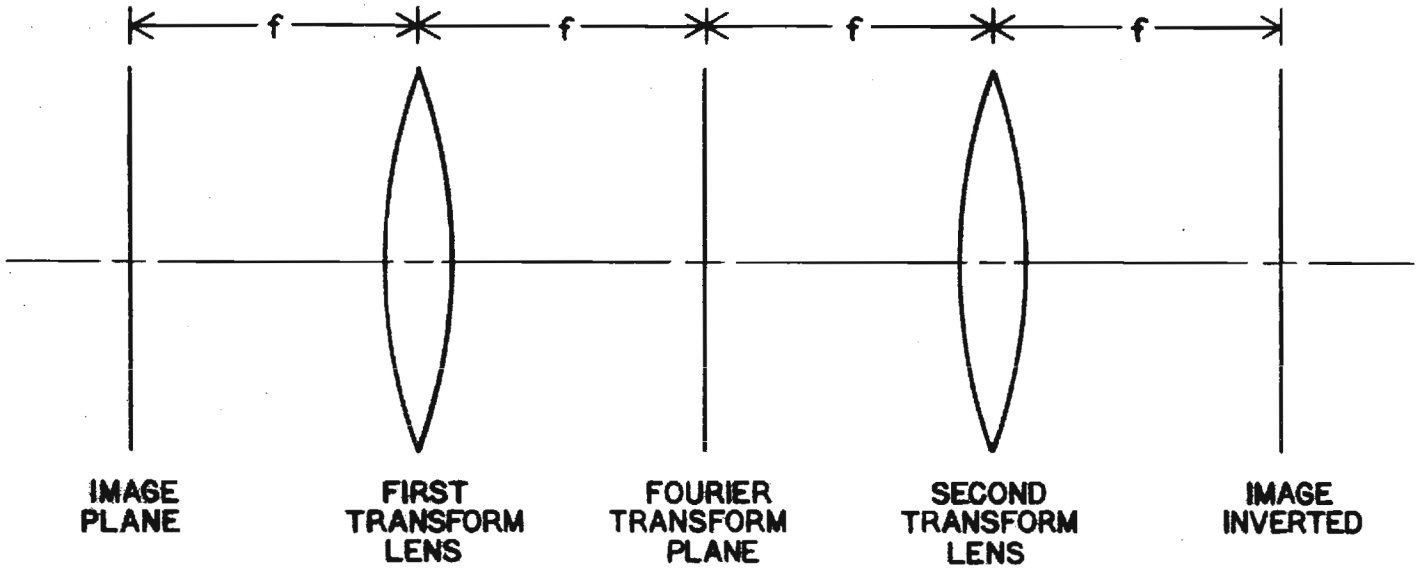

FIGURE 1. BASIC OPTICAL PROCESSOR

point depends upon the optical density of the image. To compensate for the varying optical density of the film when operating in the scanning mode, a feedback system must be employed to control the intensity of the laser beam. This allows the intensity of the correlation spot to be independent of film properties such as variation of exposure. In order to implement a parallel beam scanning system for large-image processing, it is necessary to interface a laser with a suitable random access deflector and large aperture optics.

The emphasis of the program was on the design and construction of a coherent light scanning system that was delivered, installed, and demonstrated at MSFC. This program included an intensive study to determine the optimal way of realizing the system. In addition to strictly technical considerations, the study considered such factors as cost, size, and weight. The optical beam for the scanning system was provided by a high power argon laser. The scanning system that was delivered has the following features. The laser, which has a 1.5 watt beam and operates in a single line, is capable of either random access scan over a 10 cm by 10 cm format or stationary beam operation. The random access scan positions are controllable by a digital computer with a digital-to-analog interface. A feedback system is provided such that the average light intensity of the beam remains constant to within 2% after passage through the image plane of the processor. A spatial filter with emphasis on stability is included in order to insure that the output beam is suitable for optical processing experiments over an extended period of time. The diameter of the scanned beam is adjustable from approximately 1.2 mm to 12 mm. The scanned beam is capable of processing a 10 cm by 10 cm (4" by 4") aerial photograph image.

II. OPTICAL SYSTEM DESIGN

A. Overall Approach

A schematic diagram of the optical scanning system is shown in Figure 2. The laser output (TEM_{∞} and single longitudinal mode for extended coherence) is controlled by a Pockel's effect modulator. After the modulator, the beam passes through a spatial filter, is expanded and re-collimated, and then is reduced to the desired diameter by an adjustable aperture assembly. A beam-splitter reflects a portion of the beam to be used as a reference beam in constructing holographic filters. These components are discussed in Section D, Stationary Optics.

The scanning is accomplished by a pair of orthogonal light deflecting galvanometers positioned at the focus of an off-axis parabolic mirror. The optics of the scanning operation are discussed in Section E, Scanning Optics.

B. Laser Selection

The only commercially available gas laser capable of two watt single line CW output is the argon laser using the 514.5 nm line. After lengthy considerations, the model chosen for incorporation into the laser scanner was the Coherent Radiation Model 52B. The following accessories are included in the basic laser unit:

i) Brewster angle windows for vertically polarized output;

ii) An intra-cavity etalon to extend the coherence length;

iii) An externally adjustable prism wavelength selector for selection of other argon lines.

IV) A power control unit to provide amplitude stability of the output, with power meter to monitor the laser output.

The long term power stability of the laser with power control unit is rated at less than .3% fluctuation with an integration time of one second

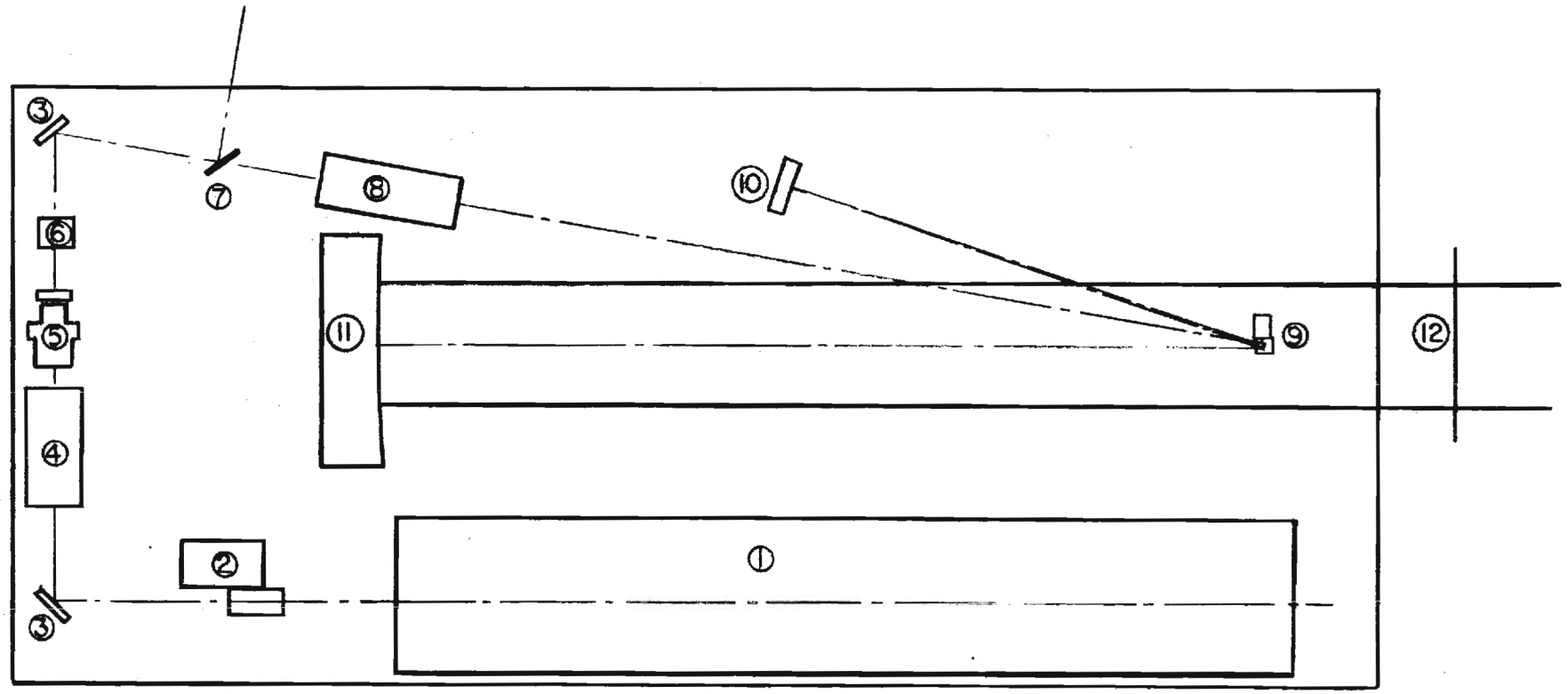

1.) ARGON ION LASER
2.) SHUTTER
3.) FLAT MIRROR
4.) POCKEL'S EFFECT MODULATOR
5.) SPATIAL FILTER COLLIMATOR ASSEMBLY
6.) APERTURE ASSEMBLY
7.) BEAMSPLITTER
8.) VARIABLE FOCUS LENS SYSTEM
9.) GALVANOMETER DRIVEN MIRROR ASSEMBLY
10.) f/4 SPHERICAL MIRROR
11.) f/3.5 PARABOLIC MIRROR
12.) FILM PLANE SHOWING SCANNED FORMAT

FIGURE 2. LASER SCANNER OPTICAL SYSTEM LAYOUT

for a ten hour period. The rated noise figure for the Model CR - 52B is less than .2% RMS in the spectral range of 10 Hz to 20 MHz.

C. Light Leveling Control System

1. Introduction

The purpose of the light leveling control system used with the optical scanner is to maintain the intensity of the light passing through the image at very nearly a constant value. This prevents the changes in film density during the scanning of a film from upsetting the threshold levels used in the correlation plane. These levels are used to make a decision as to whether or not a desired object is present in the small area of the image that the laser beam is illuminating.

Figure 3 is a simplified block diagram of the feedback control system. The laser beam is directed through the modulator to the scanning mechanism that provides scanning of the film plane. From the film, the laser beam is passed through the transform lens and to a beamsplitter just ahead of the spatial frequency transform plane to pick off a fraction of the dc component of the light passing through the image. The part of the dc component diverted from the transform plane is directed to a photodiode to sense the amplitude of the light illuminating the image. The current produced by the light intensity on the diode is converted in the preamp to a voltage by an operational amplifier current-to-voltage converter and is further amplified and level shifted to provide the proper input signal level and dc component for the modulator driver. The feedback polarity is such that an increase in the light level of the transformed image causes an increase in attenuation of the modulator, thus tending to stabilize the amplitude of the light passing through the film.

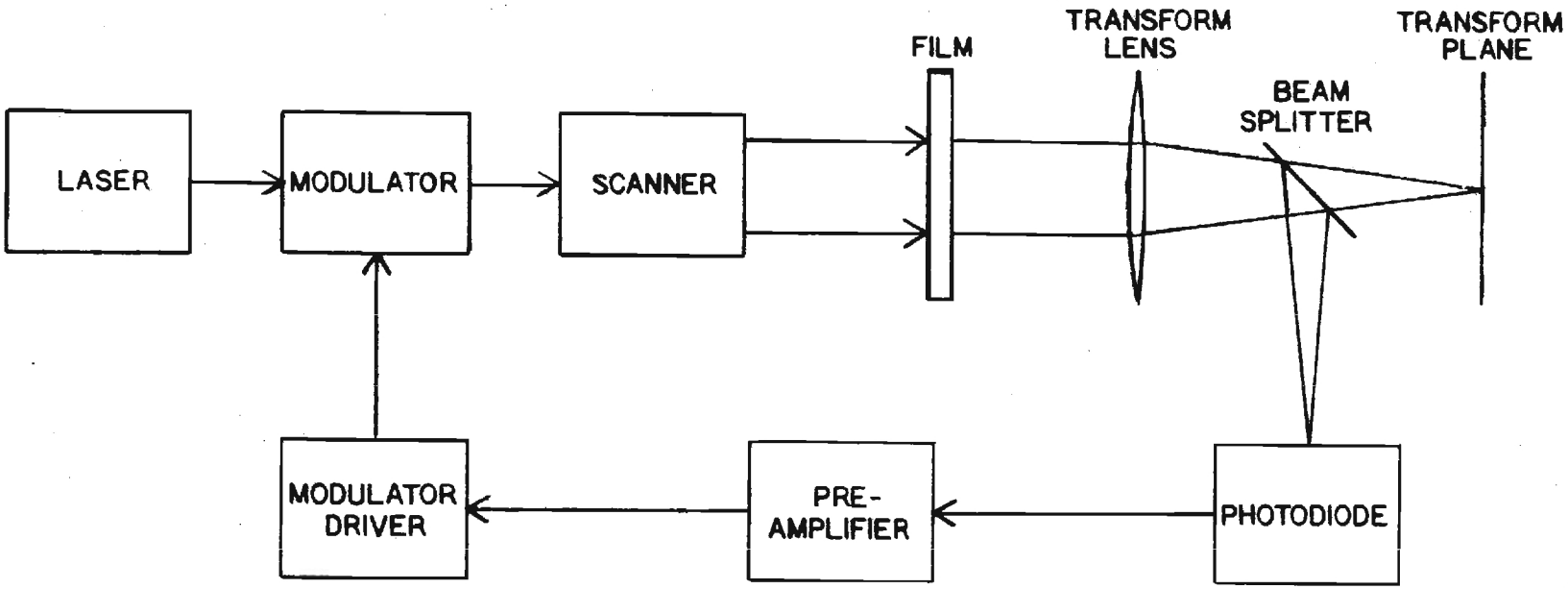

FIGURE 3. BLOCK DIAGRAM OF LIGHT LEVELING CONTROL SYSTEM

The following section will describe the feedback control system mathematically and present a computer simulation of the system using the simulation program MIMIC. This will be followed by a section that presents a more detailed discussion of the electronic circuitry, and a section that presents a brief discussion of some consideration in the use of the system.

2. Simulation of the Feedback Control System

The configuration of the feedback control system to be studied with the simulation program MIMIC is shown in Figure 4. That figure shows that a feedback voltage VF, resulting from the light on a photodiode in the transform plane, is compared with a reference voltage, VSET, to obtain the voltage to drive the modulator. In the forward portion of the feedback loop two gains are encountered. These gains, KA2 and KMD, represent the gain of the preamp and the gain of the modulator driver respectively. The modulator driver is a piece of commercial equipment (Coherent Associates Model 30B) that provides an adequate output voltage to drive the modulator for an input signal of one volt across 50 ohms. The limiter (LIM in Figure 4) in the block diagram of Figure 4 is to prevent the simulated modulator driver output voltage from reaching values that would produce a loop gain of zero. The modulator itself has an output light intensity, I, which is given by

$$I = I_o \, \mathrm{Sin}^2 \left[\left(\frac{\pi}{2} \right) \left(\frac{V_{in}}{V_{\lambda/2}} \right) \right] \qquad (1)$$

where I_o is the maximum light intensity, V_{in} is the modulator driver output voltage and $V_{\lambda/2}$ is that value of drive voltage that gives the maximum light transmission. For the modulator used in the scanner, $V_{\lambda/2}$ is approximately 115 volts. Following the modulator in the simulation is KF, the transmission gain of the film in the input plane. The output light intensity is given by I_1, the controlled variable.

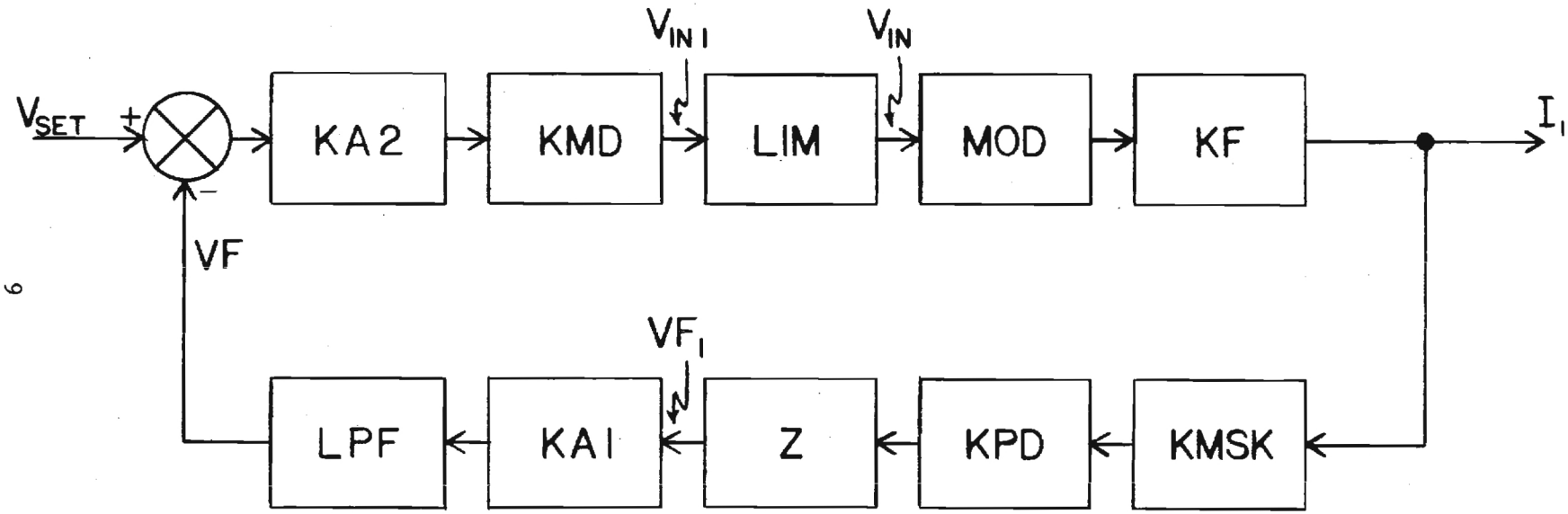

FIGURE 4. BLOCK DIAGRAM OF FEEDBACK CONTROL SYSTEM TO BE SIMULATED WITH MIMIC

In the feedback path, KMASK provides a means of accounting for the light that appears in the transform information at spatial frequencies higher than dc. The photodiode responsivity is represented by KPD, which relates the amount of current produced by the diode to a given amount of light power incident on it. This current in the impedance Z produces the feedback voltage. The gain in the feedback path ahead of the voltage comparison point is represented by KA1. The last item in the feedback loop is a low-pass filter that sets the system bandwidth. The low-pass filter output, VF, is compared in the differential circuit with VSET to produce the error voltage.

The control system was simulated using the simulation language MIMIC. MIMIC was developed at Wright-Patterson AFB in the mid-1960's for digital simulation of dynamic systems. Instruction for its use are given in the original MIMIC report.* Reference should be made to that report for a description of the details of the simulation language.

The entry of the system description into MIMIC is shown in Figure 5. The equations describing the circuit are entered into MIMIC, which sorts and integrates them for simulation of the feedback system. The first two statements are "parameter statements," which allow a solution of the system equations and reentry of a new set of parameters withour reexecuting the program. Statement 3 defines the transfer function of the modulator as

$$I_1 = KF \cdot I_o \cdot \sin^2 \left(\frac{\pi}{2} \cdot \frac{V_{in}}{V_{\lambda/2}} \right) \qquad (2)$$

where I_1 is the output light power, KF is the transmission of the film,

---

* Peterson, H. E., F. J. Sampson and L. M. Warshawsky, MIMIC-A Digital Simulation Program, SESCA Internal Memo 65-12, Directorate for Computation, Deputy for Studies and Analysis, Systems Engineering Group, Wright-Patterson AFB, Ohio, May 1965.

```
DGT*LIB.MIMIC,IS TEST
MIMIC-04.0-10/05/73-18:16:21

   1*                   PAR(KF,KA2,VSET,KMSK)
   2*                   PAR(Z,KA1,TOU)
   3*          I1       KF*I0*SIN(1.5708*VIN/VLAM2)*SIN(1.5708*VIN/VLAM2)
   4*          KMD      300.
   5*          KPD      .4
   6*          VIN1     KMD * KA2 * (VSET - VF)
   7*          VIN      LIM(VIN1,1.,114.)
   8*          VF1      KMSK * KPD * Z * I1
   9*          DT       TF / 9.
  10*          TF       200. * ( TOU / K)
  11*          K1       KA2 * KMD
  12*          K2       KMSK * KPD * Z * KA1
  13*          K        K1 * KF * I0 * K2 * (1.5708) / VLAM2
  14*          VF       INT((KA1 * VF1 - VF) / TOU, 0.)
  15*          I0       .01
  16*          VLAM2    115.
  17*                   FIN(T,TF)
  18*                   HDR(TIME,IOUT,VIN,VIN1,VF,VF1)
  19*                   OUT(T,I1,VIN,VIN1,VF,VF1)
  20*                   END

**FURTHER DIAGNOSTICS AND EXECUTION FOLLOW***

ENTER DATA NOW
  KF            KA2           VSET          KMSK
 1.00000-02    10.000        2.0000        1.00000-02


ENTER DATA NOW
  Z             KA1           TOU
 1.00000+06    10.000        1.60000-06


  TIME          IOUT          VIN           VIN1          VF            VF1
 0.00000       9.99814-05    114.00        6000.0        0.00000       .39993
 2.16922-07    9.99814-05    114.00        4478.8         .50705       .39993
 4.33844-07    9.99814-05    114.00        3150.5         .94982       .39993
 6.50765-07    9.99814-05    114.00        1990.6        1.3365        .39993
 8.67687-07    9.99814-05    114.00         977.82       1.6741        .39993
 1.08461-06    9.23665-05     94.506        94.506       1.9685        .36947
 1.30153-06    4.95237-05     57.151        57.151       1.9809        .19809
 1.51845-06    4.95197-05     57.148        57.148       1.9810        .19808
 1.73537-06    4.91503-05     56.878        56.878       1.9810        .19660
 1.95230-06    4.96240-05     57.225        57.225       1.9809        .19850

ENTER DATA NOW
  KF            KA2           VSET          KMSK
  1.0000       10.000         2.0000        1.00000-02

ENTER DATA NOW
  Z             KA1           TOU
 1.00000+06    10.000        1.60000-06


  TIME          IOUT          VIN           VIN1          VF            VF1
 0.00000       9.99814-03    114.00        6000.0        0.00000       39.993
 2.16922-09    9.99814-03    114.00        4374.5         .54184       39.993
 4.33844-09    9.99814-03    114.00        2751.2        1.0829        39.993
 6.50765-09    9.99814-03    114.00        1130.1        1.6233        39.993
 8.67687-09    1.76316-04      9.8055        9.8055      1.9967         .71326
 1.08461-08    5.27005-05      5.3194        5.3194      1.9982         .21080
 1.30153-08    5.00724-05      5.1849        5.1849      1.9983         .20029
 1.51845-08    4.99536-05      5.1787        5.1787      1.9983         .19981
 1.73537-08    4.99570-05      5.1789        5.1789      1.9983         .19983
 1.95230-08    4.99570-05      5.1789        5.1789      1.9983         .19983
 2.16922-08    4.99570-05      5.1789        5.1789      1.9983         .19983
```

FIGURE 5. MIMIC Program Listing

V_{in} is the input voltage, and $V_{\lambda/2}$ is the voltage that gives maximum light transmission. Statement 4 of the program defines the voltage gain of the modulator driver. Next, the light power to photodiode output current transfer gain is defined as KPD = 0.4. V_{in1}, the input voltage to the limiter, is obtained as the product [KMD • KA2 • (VSET-VF)], where KMD is the voltage gain of the modulator, KA2 is the preamplifier voltage gain in the forward portion of the loop, and (VSET - VF) is the error voltage. Statement 7 defines a voltage limiter with limit voltages of 1 and 114 volts, which prevents the drive voltage on the modulator from crossing over the points of zero slope on the sine squared modulator transfer characteristic. Next, VF1 is defined as

$$VF1 = KMSK \cdot KPD \cdot Z \cdot I1 \ , \tag{3}$$

where KMSK specifies the loss of light power to portions of the transform plane other than the dc component, KPD is the photodiode responsivity in amperes per watt, Z is the impedance into which the photodiode operates, and I1 is the intensity of the output light after having passed through the modulator and film. The next two statements define the time interval at which the output is printed, DT, and the time at which the solution of the problem is stopped, TF. Note that TF is defined in terms of the circuit time constant TOU. Statement 11 defines K1 as the product of the preamp gain in the forward loop, KA2, and the gain of the modulator driver KMD. Next K2 is defined as

$$K_2 = KMSK \cdot KPD \cdot Z \cdot KA1 \ , \tag{4}$$

which multiplies the gains in the feedback loop. The thirteenth statement defines the small signal open loop gain as

$$K = K1 \cdot K_F \cdot I_o \cdot K_2 \cdot \frac{\pi}{2V_{\lambda/2}} \ . \tag{5}$$

The only use made of this gain term is in the calculation of the circuit time constant TOU.

Next, the low pass filter in the feedback loop is defined. This is a simple RC filter with a transfer function given by

$$\frac{E_o}{E_i} = \frac{1}{1 + sRC} \tag{6}$$

where E_i is the input voltage to the filter, E_o is the output voltage and RC is the filter time constant. This can be put in the form

$$\dot{e}_o = \frac{e_i - e_o}{RC} \tag{7}$$

Statement 14 is obtained by substituting the feedback system parameters in the above equation and integrating the right hand side using zero initial conditions:

$$VF = \int \frac{(KA1 \cdot VF1 - VF)dt}{TOU} \tag{8}$$

The next two statements define values chosen for the intensity of illumination, I_o, as 0.01 watt and $V_{\lambda/2}$ for the modulator as 115 volts.

The next four statements are instructions for execution of the program. The first is the finish time statement, the second a heading statement for output data, the third the statement that defines variables to be printed out, and last, the end statement.

Examples of the execution of the program are given in Figure 5 after the "Enter Data Now" statement. First the entry of data required by the two parameter statements is shown. The data entered were KF = 0.01, KA2 = 10., VSET = 2., KMSK = 0.01, Z = 10^6, KA1 = 10., and TOU = 1.6×10^{-6}. The parameters represent, in order, a film transmission of 0.01, a forward loop preamplifier gain of 10, a set voltage of 2 volts, a loss of light factor in the transform plane of 0.01, a load impedance for the photodiode of 1 megohm, a forward loop preamplifier voltage gain of 10, and a filter time constant of 1.6×10^{-6} (filter cut off frequency of 100 KHz). The

solution gives the time, the light intensity out, and four voltages at points around the loop. Another complete solution was obtained with only the parameter KF changed. KF was changed to 1 to represent complete transmission of the light through the film. Of interest are the output intensity IOUT, and VIN, the voltage applied to the modulator. For the case of KF = 0.01, IOUT was 4.962×10^{-5} and VIN was 57.23 volts while for KF = 1, IOUT was 4.996×10^{-5} and VIN was 5.179 volts. Thus, for a change in film transmission of 100:1, the output intensity changed only approximately 0.7 percent.

The simulation program was used to verify the operation of the feedback system concept and to obtain a feel for how it performed. Adjustment of the system in the laboratory was much easier with the knowledge gained from the simulation.

3. Circuit Mechanization

The electronic portion of the feedback control system was constructed using some commerically available components and some components that were constructed. The electronic portion of the system consisted of a United Detector Technology type PIN-5 photodiode, a preamplifier, and a modulator driver. No circuit detail data was available on that unit. The specification indicated that a one volt peak-to-peak input results in a 230 volt peak-to-peak output. The bandwidth of the modulator was indicated to be dc to 3 MHz when driving a modulator through 6 feet of cable. The input impedance was specified to be 50 ohms.

A preamplifier was constructed to provide the interface between the photodiode and the modulator driver. Figure 6 is a schematic diagram of the preamplifier, which uses two Fairchild μA715 wideband operational amplifiers. The first of these is a current-to-voltage converter connected to

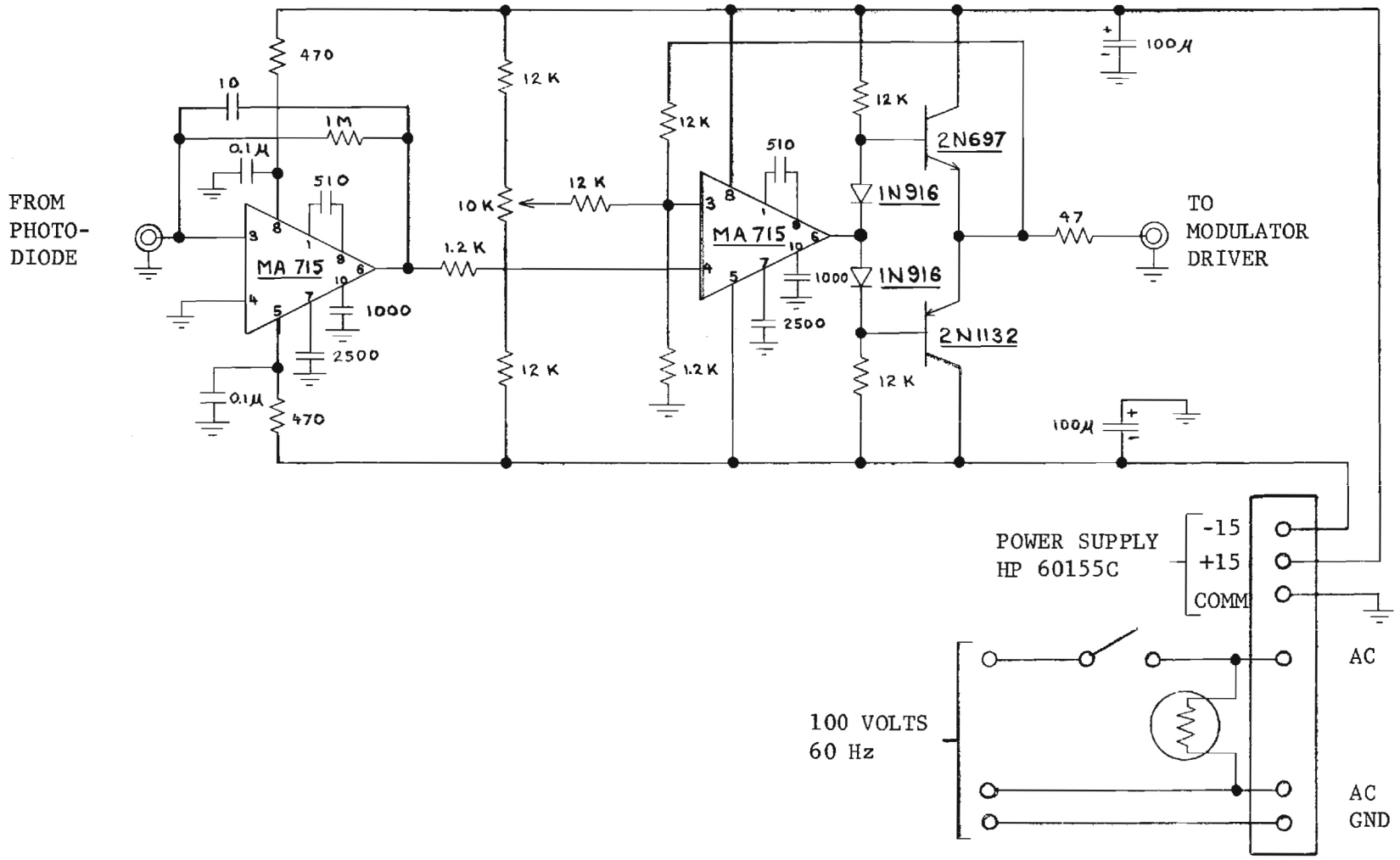

FIGURE 6. SCHEMATIC DIAGRAM OF PREAMPLIFIER

the photodiode through several feet of coaxial cable. The photodiode is operated without bias, simplifying the equipment that is located in the optical setup. The low-pass filter discussed in the simulation of the system is made up of the photodiode, the interconnecting cable, and the input impedance of the current to voltage converter.

The second operational amplifier in the preamplifier is a noninverting amplifier with a gain of approximately 10. This amplifier has included in its feedback loop a complementary symmetry emitter follower to provide the drive current for the 50 ohm input impedance of the modulator driver.

Plus and minus 15 volt power supplies for the preamplifier are obtained from a Hewlett-Packard Model 60155C dual power supply located on the same rack panel as the preamplifier.

4. Adjustment of the Feedback System

Before actual testing of the system is performed, several immediate observations about the operation of the system can be made. First, since the slope of the sine squared transfer characteristic of the modulator goes to zero at zero volts and 115 volts drive voltage, the loop gain falls to zero at these points. Thus, it is better to operate the light leveling system so that the region of operation of the modulator is near its center linear portion where the loop gain is the highest.

The intensity of the light on the photodiode controls its output current and thus the voltage developed in the current-to-voltage converter, thereby effecting the loop gain of the system. A tighter control system will be obtained for higher light intensities from the laser. These considerations were verified by laboratory experience.

D. Stationary Optics

The beam of light leaving the laser and being modulated by the feedback system must be "treated" before entering the scanning optics. The components described in this section are, referring back to Figure 2, the shutter, flat mirrors, spatial filter, collimating lens, and aperture assembly.

1. Shutter Design

The operation of the scanner in an overall hybrid-optical-digital pattern analyzer may require that the beam be totally extinguished during certain cycles. Since the modulator is not capable of total extinction, it is necessary to have a fast ($\lesssim$ 1 msec) shutter capable of blocking laser beams with powers on the order of two watts. In addition to the two above basic requirements, the following considerations were also included in the choice and design of the shutter:

1) Electronic on-off control;
2) Compactness;
3) Minimum operational vibration;
4) 5 mm clear aperture;
5) Minimum scattering while extinguishing the beam;
6) Minimum cost;
7) Minimum electromagnetic noise introduced while the shutter is switching.

Three alternative choices of shutter design were considered:

1) An electro-optic shutter;
2) An electronic leaf-type shutter drived by solenoids;
3) A galvanometer driven arm with absorbent cavity.

Due to the considerations of cost, noise, compactness, and power of the beam, the electro-optic effect shutter was determined to be infeasible. The leaf-solenoid type of shutter also was eliminated because of distortion of the leaves under high power, electro-magnetic transients when triggered, vibration, and scattering. The galvanometer driven arm, in addition to being the simplest design, also offers the trade-off between vibration and response time, and was therefore incorporated into the scanner. As designed, it fulfills all requirements.

A General Scanning Model 330 was chosen for the galvanometer. The torque requirements and response time are shown in Appendix A. For the arm and cavity a balanced aluminum rod is used. The cavity is conical with six "steps" cut from the cone, with faces angled to reflect incident light onto the walls of the cavity. The arm and cavity are black anodized. The cavity was baked with an acetylene rich oxy-acetylene welding torch to deposit a very flat balck finish to further enhance the absorptivity of the cavity. The cavity and arm configuration are shown in Figure 7.

2. Flat Mirrors

To keep the scanner as compact as possible, it is necessary to fold the light path. Two flat 50 mm. diameter mirrors purchased from Oriel Corporation are used for folding the light path, as shown in Figure 2. These mirrors are specified to be flat to $\lambda/20$ over the entire surface. The mirrors mounted in cells that are positionable in two orthogonal angles. The mirror mounts also are supplied by Oriel.

3. Spatial Filter Design

To generate holographic filters and to perform the operations of convolution and correlation optically, the laser beam must be spatially filtered. The spatial filter must be very stable for long periods of

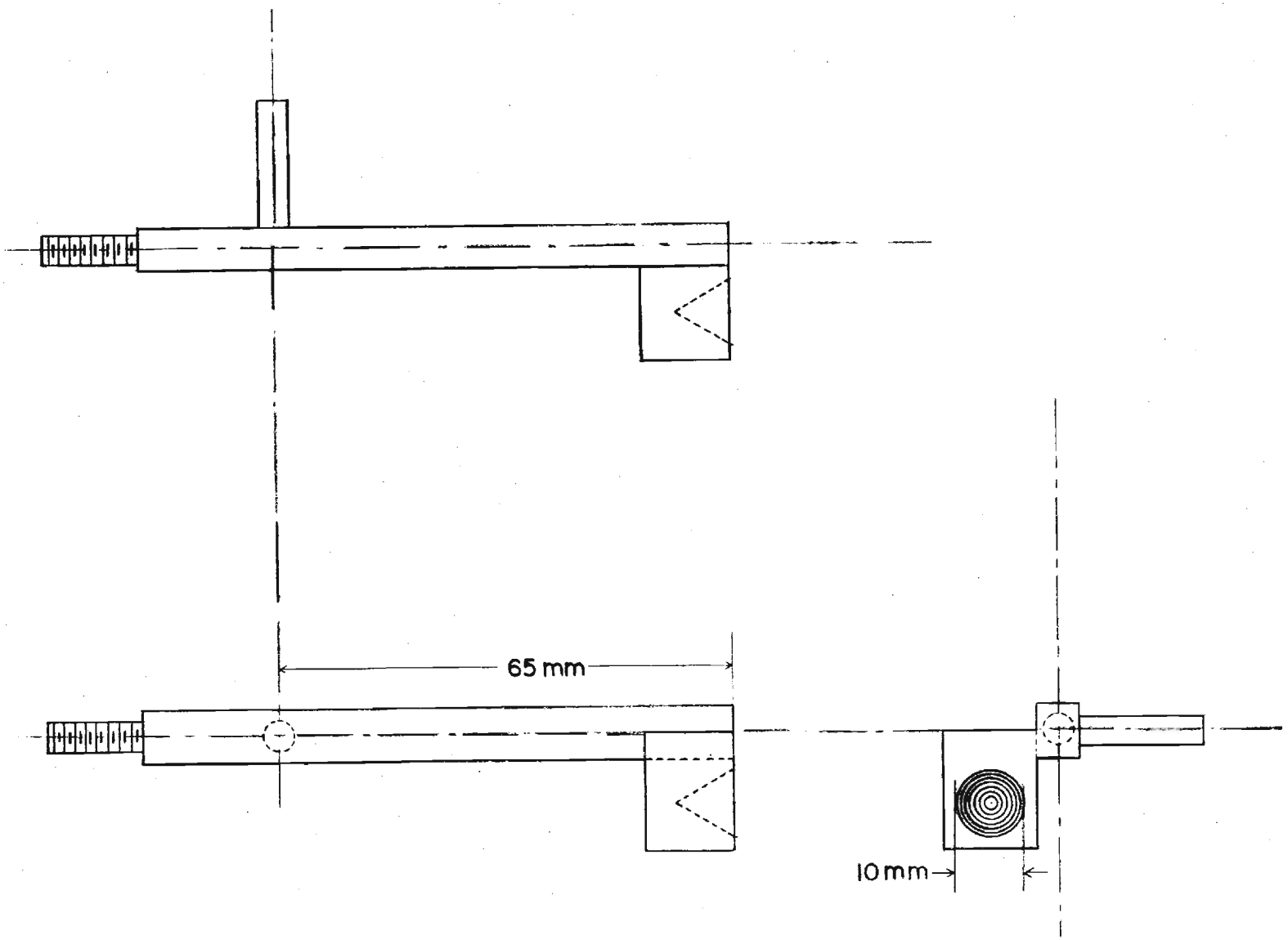

FIGURE 7. SHUTTER ARM AND CAVITY DETAIL

operation and should be relatively easy to adjust. For the spatial filter, a design developed by the Sperry Rand Corporation Space Support Division for NASA/MSFC was used. The basic design employs two lockable orthogonal tracks to position the pinhole. A lockable threaded cylinder can be used to adjust the position of the expanding lens. The design accepts expanding lenses and pinholes manufactured by Spectra-Physics, Inc.

4. Collimating Lens

The beam leaving the spatial filter is a diverging beam that must be recollimated to remain aligned with the optical path of the scanner. By proper choice of focal length and diameter, the collimating lens allows the beam to be expanded, collimated, and to maintain the same Gaussian intensity profile. A two element, 15 mm clear aperture, collimating lens, especially designed for use with a spatial filter, was purchased from the Spectra-Physics Corporation. This lens is coated for maximum transmission at 514.5 nm, the green argon laser line used in the system. This lens assembly is mounted in a threaded shaft for positioning adjustment. The mating threaded tube is aligned with the optical axis of the spatial filter assembly and mounted to the face of the spatial filter assembly. When properly aligned, the beam leaving the collimating lens is 13 mm in diameter.

5. Aperture Assembly

An important design parameter is the size and shape of the illuminated spot as it scans the image at the output of the scanner. To control the diameter of the spot, an adjustable aperture assembly is required to give the beam the proper cross section before going into the scanning optics. The spatial filter and collimator are mounted on a plate. At the end of the plate a holder for metal slides is mounted. Several slides were made for the holder and the optical axis was located on the slides. Each slide

was drilled for a different size aperture. Once the spatial filter is aligned, the beam diameter can be changed simply by removing one slide from the holder and replacing it with another slide.

To determine the range of beam diameters required, the following computations are performed:

Maximum Beam Diameter

Assuming the average automobile to be 4.8 to 6.1 meters (16 to 20 feet) long, a scanning beam effectively 10.7 meters (35 feet) in diameter will enclose the automobile with a sufficient margin to negate the design goal positioning uncertainty. The largest possible image of an automobile on the aerial photographs to be processed is assumed to be from an aircraft 305 meters (1000 feet) above the ground and photographed with a .305 m (12 inch) focal length lens.

From Figure 8,

$$\frac{10.7 \text{ m}}{\text{maximum beam diameter}} = \frac{\text{aircraft height}}{\text{focal length}} \qquad (9)$$

$\therefore$ Maximum beam diameter = 10.7 mm

To allow an additional margin, the maximum beam diameter should be 11 mm, which easily can be made with a 27/64 inch twist drill.

Minimum Beam Diameter

Due to diffraction, there exists an absolute minimum spot size. Assuming diffraction limited optics, the following calculation can be made:

From Figure 9 and making the following definitions:

D = initial beam diameter;

α = diffracted angle, from the center of the Airy disc to the first minimum, measured in radians;

λ = 514.5 nm = 2.03×10^{-5} inches;

f = focal length = 115.57 cm = 45.5 inches;

s = diameter of the beam scanning the film;

we have $S = D + 2F\alpha$

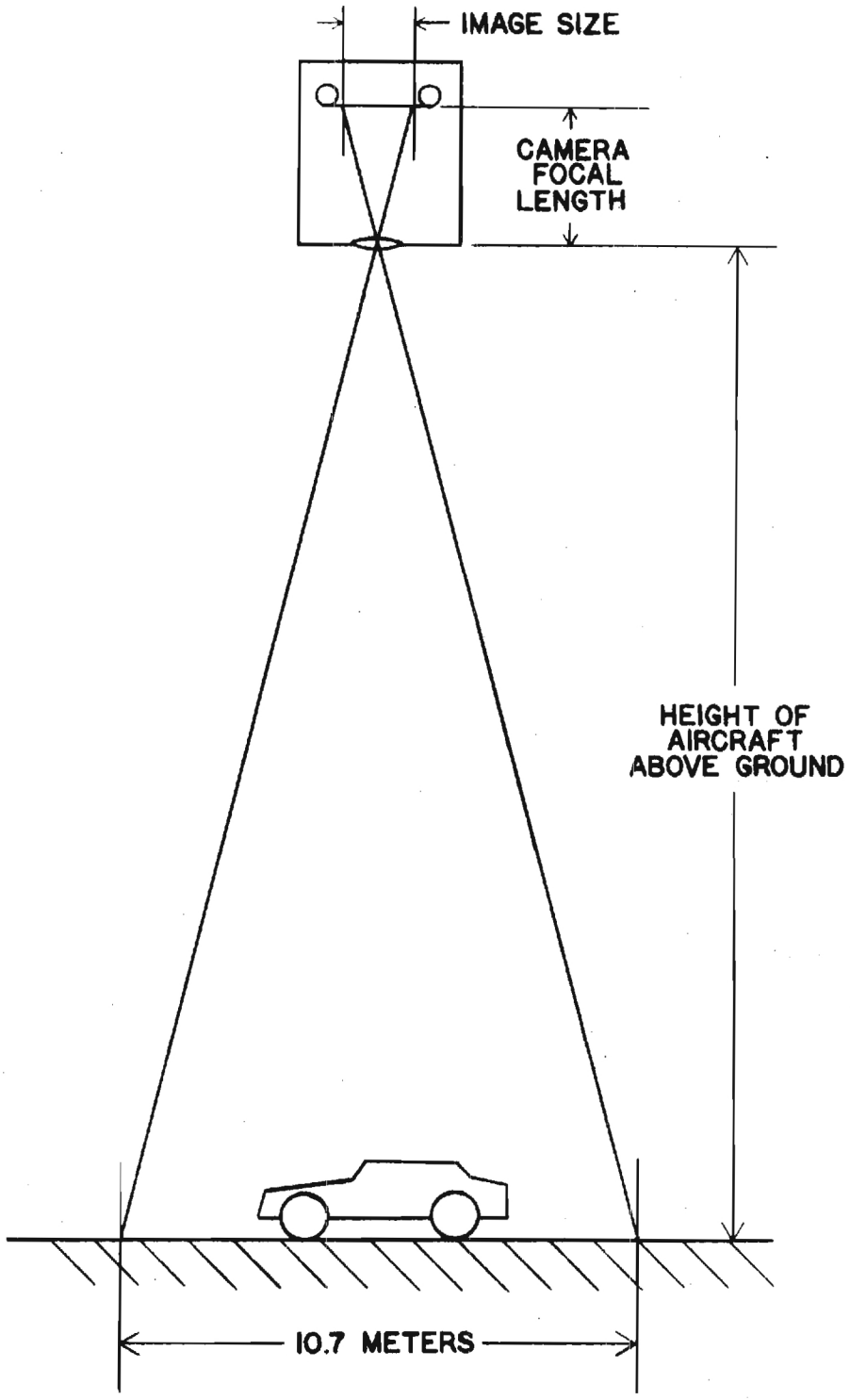

FIGURE 8. SCALING OF AERIAL PHOTOGRAPH

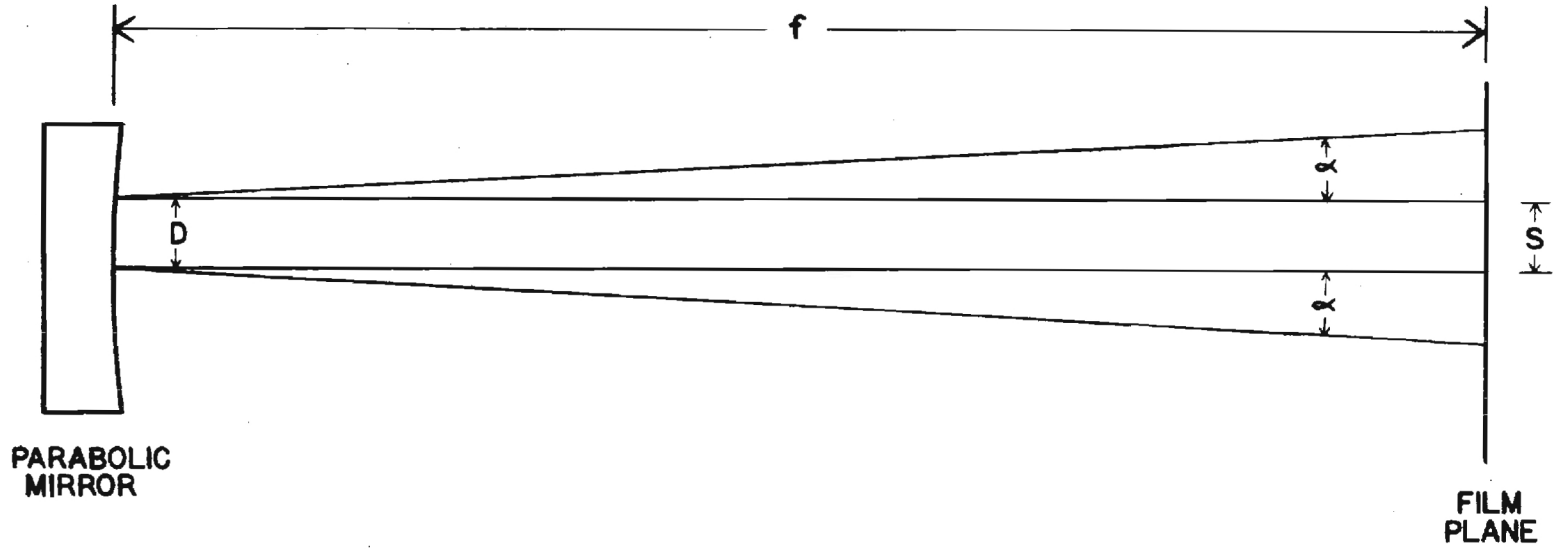

FIGURE 9. SPOT SIZE SPREADING

From the empirical rayleigh criterion for diffraction,

$$\alpha = \frac{1.22\lambda}{D} \tag{10}$$

Substituting this for α,

$$s = D + \frac{2F(1.22\lambda)}{D} \quad . \tag{11}$$

Differentiating with respect to D and minimizing,

$$\frac{ds}{dD} = 1 - \frac{2F(1.22\lambda)}{D^2} = 0 \ . \tag{12}$$

$$D = \sqrt{2F(1.22\lambda)} \quad , \quad D_{MIN} = \left[(115.57)(2)(1.22)(5.145 \times 10^{-5})\right]^{1/2} \tag{13}$$

D_{MIN} = 1.2 mm, or about 4.7×10^{-2} inches.

As the performance of our system will be less than diffraction limited, the smallest aperture shall be 1.3 mm (.052 inches) in diameter. This may be made with a #55 twist drill. The resulting spot is analogous to the 35 ft. 10.7 m scanning circle photographed with a six inch (.152 m) focal length lens at 4,000 (1220 m) ft. or a twelve inch (.305 m) focal length lens at 8,000 ft. (2440 m).

E. Scanning Optics

The scanning is accomplished by a pair of light deflecting galvanometers, driven by external electrical signals. The part of the beam that is transmitted through the beamsplitter is focused to a point by a two element variable focus lens system. This point lies on the axis of rotation of the first galvanometer mirror. By applying an electrical signal to this galvanometer, the beam is deflected in the horizontal (x) direction.

A spherical mirror is positioned such that the first galvanometer is displaced slightly from its center of curvature. The divergent beam reflected from the first galvanometer mirror falls on the spherical mirror and is focused

to a second point equally displaced from, but on the opposite side of, the center of curvature. The second light deflecting galvanometer is positioned such that its axis of rotation is orthogonal to the first galvanometer and passes through the second focus. This galvanometer is used to deflect the beam in the vertical (y) direction.

An off-axis parabolic section is used to collect the light from the y galvanometer. It is mounted with its focus on the axis of rotation of the second galvanometer, which deflects the focused point of light from the spherical mirror. The parabolic mirror collimates the beam and reflects it in a direction parallel to the optical axis. With the variable focal length lens system adjusted to have the same focal length as the parabolic section, the final scanning beam diameter will be the same as the diameter of the beam determined by the adjustable aperture assembly.

Film placed in the locus of the collimated beam leaving the parabola may be scanned by driving each galvanometer with the proper deflection signal. With no signal applied to either galvanometer, the beam is stationary and passes through the center of the 10 cm x 10 cm (4" by 4") format.

1. Zoom Lens

A two element variable focus converging lens is used to focus the collimated beam to a small diameter spot in the plane of the first galvanometer mirror. By adjusting the effective focal length of the converging lens to be equivalent to the focal length of the parabolic mirror, the diameter of the spot scanning the film can be made equal to that of the aperture inserted into the adjustable aperture assembly.

2. Parabolic Mirror

The parabola has to be large enough to allow a 10 cm x 10 cm projected square to fall on the surface with maximum separation from the

center. The 10 cm x 10 cm square is, effectively, the locus of points on the parabola that the beam must trace to scan a 10 cm x 10 cm aerial photograph. The last galvanometer lies on the optical axis of the parabola and occults the central portion of the parabola.

If a 33.0 cm diameter is chosen, assuming a separation of five cm from the center, the clearance of the extreme corners of the 10 cm square is given by, from Figure 10,

$$D = 16.5 - \sqrt{(15.0)^2 + (5.0)^2} = 0.688 \text{ cm} \approx 7 \text{ mm} \qquad (14)$$

This is reasonable, as these are worst case numbers. If the performance of the outer edge of the mirror is insufficient, it is possible to move the projected square closer to the center of the mirror.

Focal Length Considerations

A short focal length allows the laser scanner package to be more compact. This would be ideal except that the shorter focal length mirrors have deeper sagittas. As more glass must be removed and the testing is more difficult for this type of mirror, the cost is higher.

To determine a reasonable trade-off, the following computations are made:

The difficulty in testing a "fast" parabolic mirror is due to the deviation of the surface from that of a sphere. This deviation is a common gauge used by optics manufacturers for estimating costs. From Figure 11, we make the following definitions:

$$R = \begin{cases} R = \text{Radius of the mirror;} \\ F = \text{Focal Length;} \\ y_s = \text{Sagitta of the spherical;} \\ y_p = \text{Sagitta of the paraboloid;} \\ \Delta y = y_s - y_p; \\ \Delta s = \text{Deviation from the sphere.} \end{cases}$$

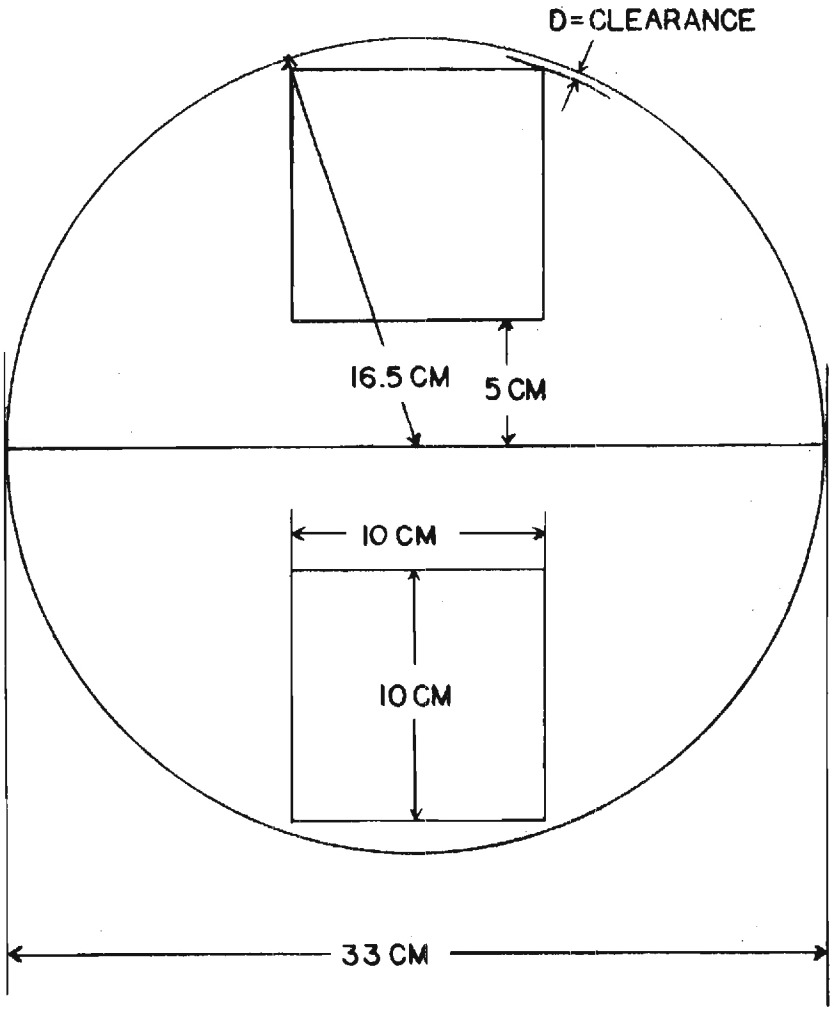

FIGURE 10, FORMAT PROJECTION ON PARABOLIC MIRROR SURFACE

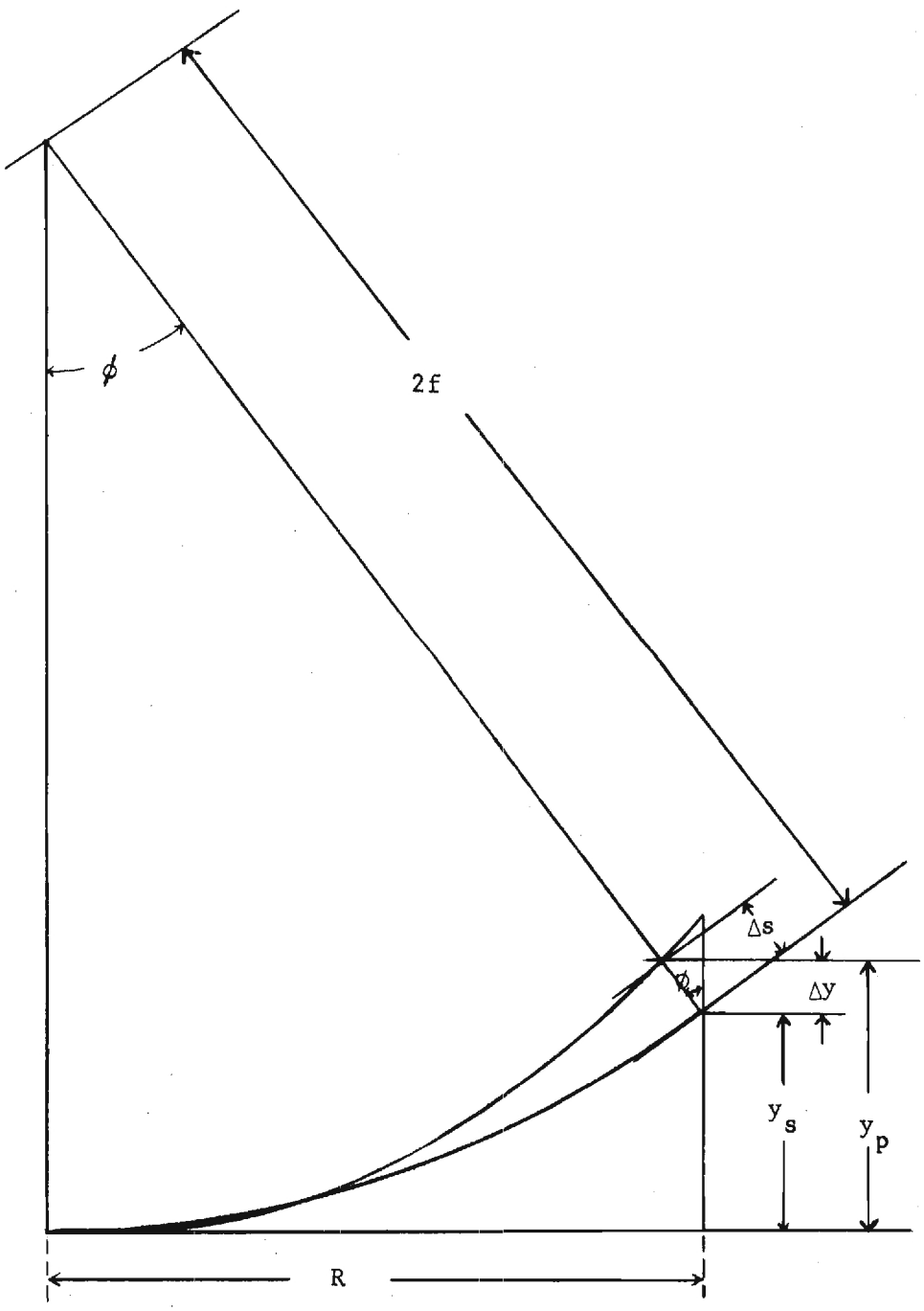

FIGURE 11. DEVIATION OF PARABOLA FROM A CIRCLE

For a circle tangent to the abscissa at the origin,

$$y_s = 2f - \sqrt{4F^2 - R^2} \tag{15}$$

For a parabola tangent to the abscissa at the origin,

$$y_p = \frac{R^2}{4F} \quad \text{and} \quad \Delta_y = y_s - y_p = 2f - \frac{R^2}{4F} - \sqrt{4F^2 - R^2} \tag{16}$$

Expanding $\sqrt{4F^2 - R^2}$ for $R^2 \ll 4F^2$

$$(4F^2 - R^2)^{1/2} \cong 2f - \frac{R^2}{4F} - \frac{R^4}{64F^3} \; . \tag{17}$$

Substituting in Δ_y ,

$$\Delta_y = 2f - \frac{R^2}{4F} - (2f - \frac{F^2}{4F} - \frac{R^4}{64F^3}) = \frac{R^4}{64F^3} \; . \tag{18}$$

From Figure 11, $\Delta_s = \Delta_y \cos \phi$ and $\frac{R}{2f} = \sin \phi$

$$\Delta_y = \frac{R^4}{64F^3} = \frac{R}{8} \sin^3 \phi \tag{19}$$

$$\Delta_s = \frac{R}{8} \sin^3 \phi \cos \phi \tag{20}$$

From the previous section, it was determined that

$R = 16.5$ cm

by substituting this value of R in the expression Δ_s and plotting Δ_s as a function of ϕ, Figure 12 was drawn.

From these data it is determined that, for resonable cost, the parabola should not deviate from a sphere by more than 15 wavelengths. This corresponds to approximately F/3.3. Bearing this in mind and examining the light deflecting galvanometers that are commercially available, a design deflection angle of eight degrees is chosen. This angle is not the angle ϕ measured from the center of curvature, but the full deflection

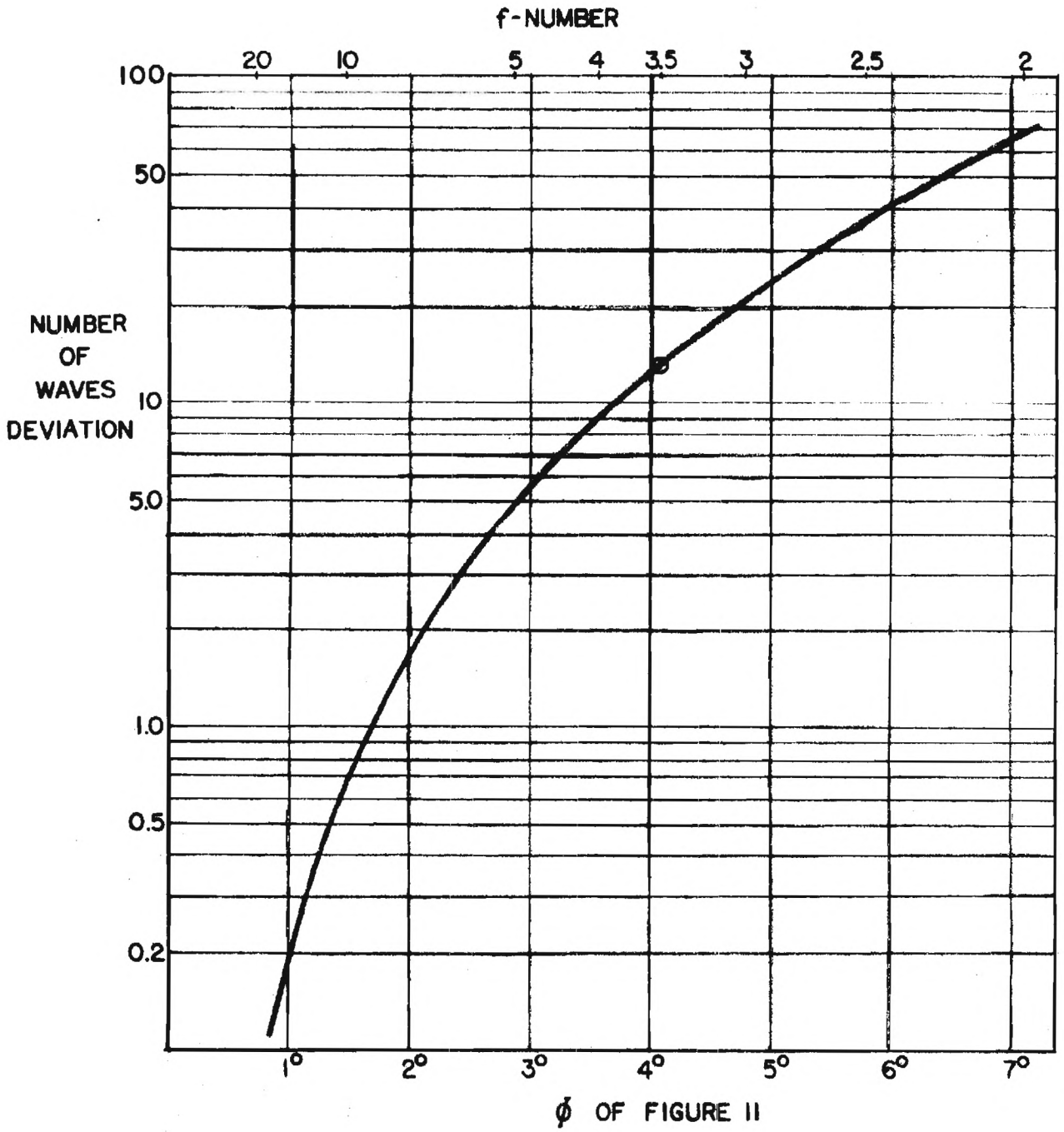

FIGURE 12. DEVIATION OF PARABOLIC MIRROR FROM A SPHERE

measured from the focus.

$$10 \text{ cm} = 2F \sin 3^\circ$$

$$F = \frac{10}{0.105} = 95.53 \text{ cm minimum} \qquad (21)$$

To reach a trade-off from both considerations a focal length of 115 cm, F/3.5 is chosen.

3. Spherical Mirror

Diameter Considerations

From the six degree scan angle of the light deflecting galvanometers, it is apparent that the spherical mirror must subtend at least that planar angle. The light deflecting galvanometers will operate in the proximity of the center of curvature of the sphere.

From Figure 13, $D = 4F \sin 3^\circ = F(.209)$

Therefore the F-number $(\frac{F}{D})$ of the spherical mirror must be less than $\frac{1}{0.209}$ or approximately F/5. Due to the possibility of the edge deforming after mounting, F/4 is a reasonable decision.

Focal Length Considerations

The primary considerations for the focal length of the spherical mirror are as follows: (1) the cost, (2) the space required, (3) the angle off-axis of the light deflecting galvanometers. For an F/4 mirror low cost implies short focal length or a smaller mirror. To minimize space requirements within the package, a short focal length would be optimum.

Spherical mirrors exhibit increasing coma as one attempts to image at an angle from the optical axis. Therefore it is imperative that the angle off-axis be minimized. As a design figure, a distance of 4 mm is chosen for the separation of the two axes of rotation of the galvanometer mirrors.

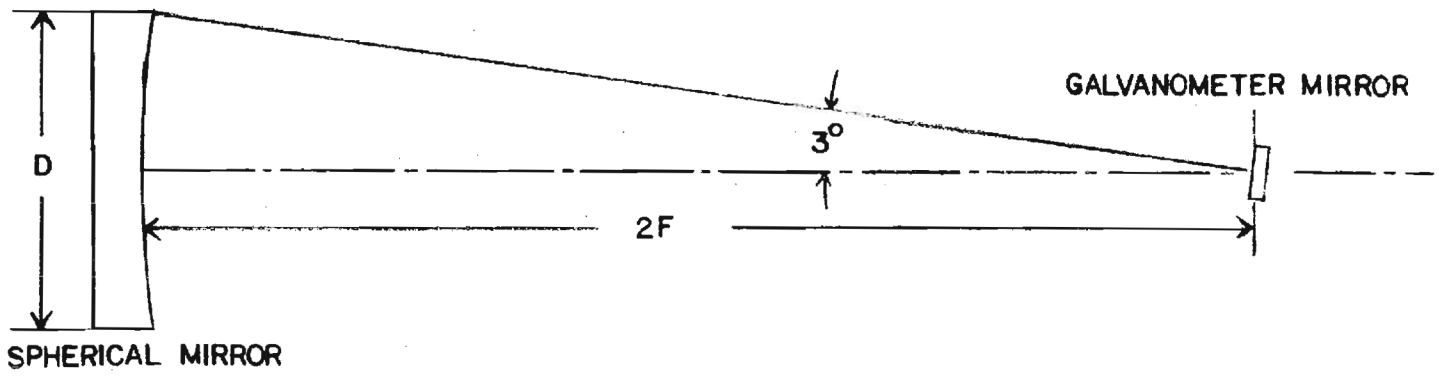

FIGURE 13. SPHERICAL MIRROR DIAMETER DETERMINATION

The angle off-axis is then

$$\alpha = \sin^{-1} \frac{0.2}{F}$$

By plotting α as a function of the focal length, Figure 14 is obtained. From the data, a focal length of 30.5 cm appears to be a reasonable off. For an F/4 mirror this allows a low cost 7.6 cm (3 inch) diameter blank.

4. Figure of Mirrors

Due to the changes in temperature within the package, cost considerations, mounting considerations, and the lack of equipment to verify the manufacturer's claims, a figure of $\lambda/10$ RMS is specified for both the parabolic and the spherical mirrors. As a result, diffraction limited performance will probably not be obtained.

5. Galvanometers

The two galvanometers are mounted with their axes of rotation orthogonal to each other, as described in the introduction to this section. The galvanometers are General Scanning Inc. Model 108 PD and use Model RAX-100 drivers. The galvanometers were chosen because of an access time of 2 msec, with minimum hysteresis error, and a maximum full angle scan of 8°. The spherical mirror is positioned 60.9 cm from the first galvanometer. In order to trace a 10 cm x 10 cm scanning area, the galvanometers scan through a full angle of 5.03°.

F. Interface

The great versatility of the coherent light scanner lies in the fact that the scanning operation can be entirely controlled by computer. The control signals from the computer are in the form of 5 volt signals (TTL) using a two's complement code. The control signal is fed into a D/A

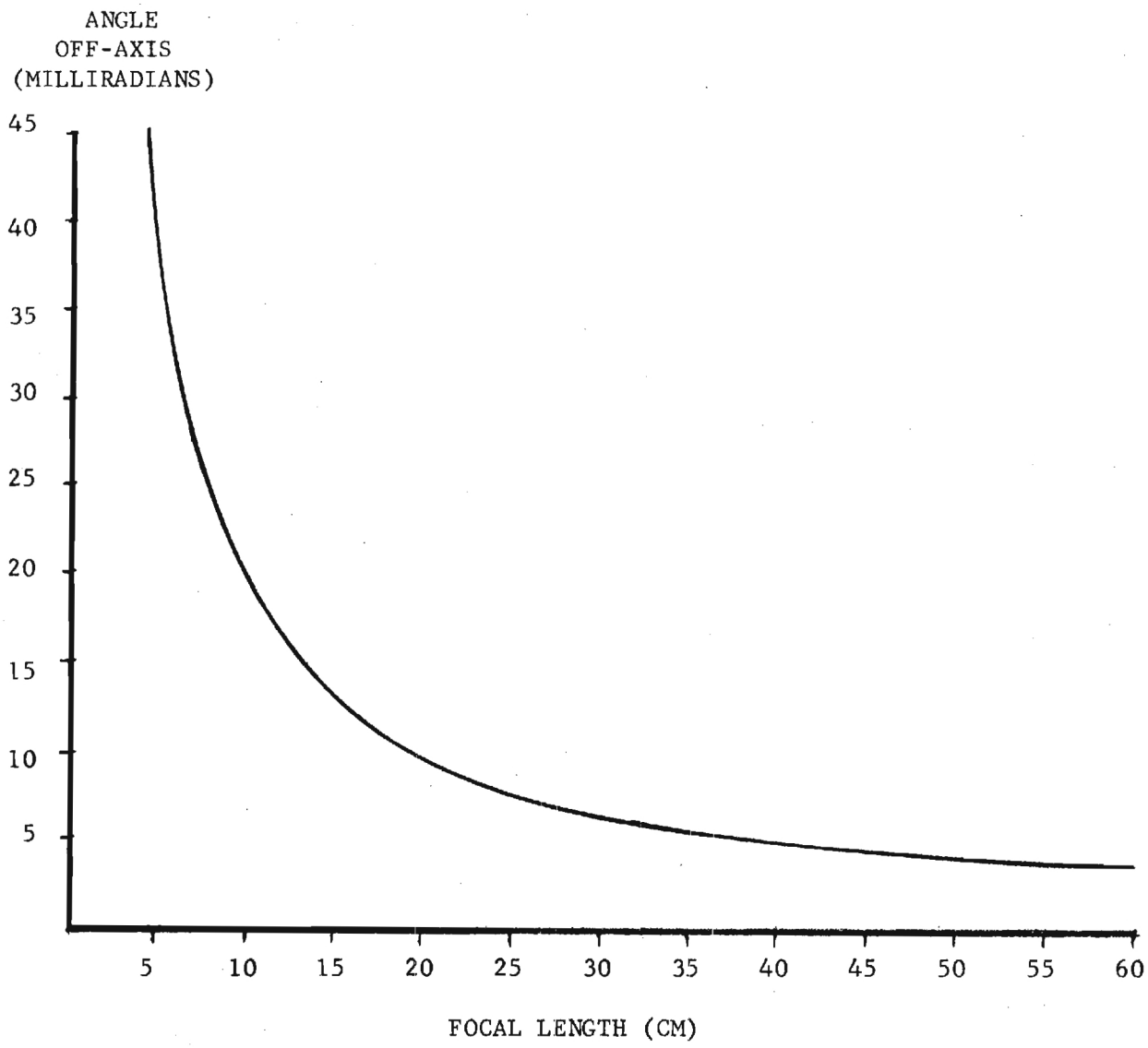

FIGURE 14. SPHERICAL MIRROR FOCAL LENGTH CONSIDERATIONS.

converter, with an analog signal level range of $\pm$ 1 volt. The analog signals from the D/A is used as the input to the model RAX-100 drivers supplied by General Scanning. These drivers have a gain adjust knob that can be used to convert the maximum voltage input to a $\pm$ 1 ampere current that causes the full galvanometer deflection of a half angle of $\pm$ 4° for the Model 108 PD scanning galvanometers, or $\pm$ 15° for the Model 330, used as the shutter.

III. SYSTEM OPERATION

A. Laser Operation

The laser requires a supply of cooling water, at a rate of approximately 3.8 liters/min (2.5 gpm) @ 2.07 x 10^5 nt/m^2 (30 psi). The power required to operate the power supply is 208/120 V, 3-phase, 50 amp, at 50/60 Hz. The laser should be carefully operated in accordance with the manufacturer's operation manual.

B. System Alignment

The following procedure can be used to ensure proper alignment of the laser scanner.

1) Place the laser on the plates mounted on the surface of the Unidek plates that have been specially designed to accommodate the laser head pads. Turn the laser on and allow it to warm up. Take a scale at least 25 cm (10 inches) long and mount it on a block so that the height of the beam above the surface can be measured. Using this scale to measure, adjust the height of the laser pads until the beam is parallel to the surface and is 13.65 cm (5-3/8 inches) above the surface of the Unidek plate.

2) Position the two flat mirrors on the Unidek surface. Use the scale to adjust the mirrors so that the beam remains 13.65 cm above the surface and parallel to the surface.

3) Position the galvanometer assembly (with the galvanometer drivers on, and with no zero and no address signals) approximately 20 cm from the desired position of the parabola and in line with the optical axis of the parabola. Adjust the second flat mirror so that the beam falls on the x galvanometer. By turning the two knurled knobs on the galvanometer mount assembly, extend the two galvanometers until their mirrors are almost touching.

4) Install the shutter.

5) Install the modulator, as described in Section III. C. Position the modulator as close to the first flat mirror as is possible.

6) After removing the pinhole and all optics, install the spatial filter as close to the laser as possible. There should be no aperture in the aperture holder. By eye, align the case so that the beam passes through the center of the aperture formed by the threaded hole for the expanding lens and the aperture formed by the hole for the mounted pinhole. If the x galvanometer mirror centerline of the case is not parallel to the beam, use .025 mm (.001 inch) shim stock to correct this.

Insert the expanding lens and fine adjust the case position until the beam has maximum brightness along the optical axis. Insert the pinhole and place a piece of frosted transparent tape over the front of the pinhole mount. Adjust the position of the pinhole until a bright spot of light is seen on the tape. Change the separation between the expanding lens and the pinhole by turning the large knurled collar at the back of the spatial filter case. By iteratively re-positioning the pinhole and focusing the expanding lens, one eventually obtains a uniformly illuminated circle of maximum brightness. When this is obtained, lock the pinhole position adjustments.

Install the collimating lens mount on the front of the spatial filter case. Adjust the position of the collimating lens until the beam is collimated. Lock the collimator focus adjustment with the locking ring on the collimator mount.

7) Install the beamsplitter and adjust it to obtain the proper ratio of object beam intensity to reference beam intensity.

8) The beam falling on the galvanometer assembly is then slightly displaced. Reposition the galvanometer assembly so that the transmitted beam is centered on the x galvanometer mirror.

9) Carefully position the off-axis parabola 115.57 cm (45.50 inches) from the y galvanometer mirror. By eye, position the focus of the parabola so that it falls on the y galvanometer mirror.

10) Install the zoom lens assembly. Align the small rail with the beam from the beamsplitter. Place the lenses on the rail and fine adjust the rail position until the beam passes through the center of both lenses. Adjust the rail position and lens separation until the smallest spot (center of the waist region) falls on the center of the x galvanometer mirror. It may be necessary to use smoke or a white card to find the waist.

11) Loosen the setscrew on the base of the x galvanometer and swing the mirror until the reflected (diverging) beam forms an angle of 15° to 20° to the right of the incident beam.

12) Position the spherical mirror along the reflected beam, 61 cm (24 inches) from the x galvanometer mirror. If the beam from the x galvanometer falls above or below the center line of the sphere, use .051 mm (.002 inches) shim stock between the base plate and brackets of the galvanometer mount assembly to correct this.

13) Adjust the spherical mirror mount until the beam reflected by the spherical mirror falls on the center of the y galvanometer mirror. If the

beam is not focused to the smallest spot on the y galvanometer mirror, the zoom lens focus should be rechecked. If that is correct, move the spherical mirror until the smallest spot on the y galvanometer mirror is obtained.

14) Position the scale on the center of the bottom edge of the parabola. Place a piece of tape on the scale such that the edge of the tape is 23.813 cm (9-3/8 inches) above the surface of the Unidek plate.

15) Loosen the setscrew at the base of the y galvanometer, and swing the y galvanometer mirror so that the beam reflected from the y galvanometer mirror is bisected by the bottom edge of the parabola. It is not necessary for the beam to fall on the parabola, because this is to be corrected in Steps 16 and 17. Estimate the proper height of the beam and tighten the setscrew.

16) Loosen the setscrew on the x galvanometer swing just enough to allow moving it by hand. Loosen the locking screw that locks the galvanometer mount assembly to the plate that is mounted to the surface of the Unidek plate. Angle the galvanometer mount assembly just enough to keep the beam from the x galvanometer falling on the sphere. If the beam from the y galvanometer has moved closer to the center of the parabola, proceed with Step 17. If it has not, angle the mount in the opposite direction.

17) Swing the x galvanometer by hand so that the beam falls on the opposite edge of the sphere. Angle the entire galvanometer assembly again until the beam from the y galvanometer falls on the center of the bottom edge of the off-axis parabola, or until the beam from the x galvanometer no longer falls on the sphere. Continue this process until the beam from the y galvanometer falls on the center of the sphere. Readjust the assembly angle and lock both adjustments. If the sphere was set too far from the incident beam in Step 11, the x galvanometer may occult the beam. If so, return to Step 11, reposition the sphere and continue with Step 12.

18) Since the x and y galvanometer mirrors have been slightly moved, the foci of the zoom lens and spherical mirror should be rechecked. The beam from the y galvanometer should be half on the mirror and centered on the bottom edge of the parabola.

19) Place the largest aperture in the adjustable aperture assembly, being certain to record the diameter of the aperture. Slightly adjust the zoom lens so that the beam waist still is falling on the x galvanometer, and that the diameter of the beam falling on the parabola is the same as that of the aperture. Recheck the focus of the sphere. If the zoom lens focus is correct, the sphere should not have to be adjusted. (This step requires two people, one to measure the spot diameter, and the other to adjust the zoom lens.)

20) Adjust the two orthogonal angles of the parabola mount until the beam reflected from the parabola passes over the y galvanometer. (The beam from the y galvanometer should still be centered on and bisected by the bottom edge of the parabola.) The straight bottom edge of the reflected beam should bisect the focused spot formed on the y galvanometer mirror by the beam from the spherical mirror.

21) Check the collimation of the beam by moving as far from the parabola as possible. Move the parabola toward or away from the y galvanometer as necessary until the beam is collimated, maintaining the beam position relative to the y galvanometer mirror. Lock the parabola in place.

22) Place a piece of tape on the mounted scale exactly 23.813 cm (9-3/8 inches) above the mounting surface. Loosen the y galvanometer set-screw and raise the beam until it is bisected by the tape when the scale is centered relative to the bottom edge of the parabola. The beam is then in its "no signal" position, the center of the 10 cm x 10 cm format.

23) By moving a screen down the beam leaving the parabola, one notices that there is a position where the aperture is most sharply defined. This is the position of the film plane. This position may be varied by changing the distance between the zoom lens and the collimating lens. Careful consideration should be given before doing this, however, because one must begin again at Step 6 once the spatial filter is moved. Only in cases of film transport mounting problems would this be reasonable.

Once the film plane has been determined, the scanner is aligned.

C. Feedback System Adjustments

The following procedure can be used to adjust the modulator and feedback system for proper operation.

Adjust the position of the modulator until the laser beam passes through the center of the front and rear apertures of the modulator assembly. Rotate the modulator until a symmetrical "brush" beam pattern appears. This should correspond to the position of maximum beam extinction with no signal applied to the modulator. Turn on the bias voltage and fine adjust the modulator for maximum extinction. Monitor the photodiode and adjust the feedback amplifier gain until $\pm$ 1 volt maximum signals are applied to the modulator driver during scanning. The points of maximum and minimum beam extinction should correspond to portions of the film having minimum and maximum optical density, respectively.

D. Considerations for Laser Operation at Wavelengths other than 514.5 nm

If the laser is tuned for operation at a wavelength other than 514.5 nm, the modulator, spatial filter, beam splitter, zoom lens, spherical mirror, galvanometer mirrors and parabola must be slightly adjusted, approximately in the above order. This is because of the chromatic aberration present in

the expanding and collimating lenses of the spatial filter, the dispersion of the beamsplitter material, and chromatic aberration of the zoom lens.

Because of coatings that are maximized for transmission at the 514.5 nm line, specular reflections are increased. For safety reasons, these should be blocked.

IV. SYSTEM EVALUATION

A. Measurement of Beam Cross Section

The following measurements were conducted at the Marshall Space Flight Center, Astrionics Laboratory (the sight of installation, S & E - ASTR - IA) from December 10 to 14, 1973. To measure the beam cross-section, a scanning device was constructed by modifying a precision traveling microscope. The traveling microscope consisted of three Velmex Unislide stages mounted orthogonally with the housing for the microscope optics mounted on the vertical stage. The entire assembly was locked in place by a large (NRC Model 200) magnetic base. Each slide was driven by a precision ground 1/4 - 40 shaft. The position was read by a scale on the stage to 0.1 inches and a two inch diameter micrometer drum with vernier to 0.0001 inches.

To convert the traveling microscope to a scanning device, two modifications were performed. The optics were removed from the housing and the housing was reversed. A UDT PIN-10 photodiode was mounted in the position of the eye piece tube. A circular aperture approximately 200 microns in diameter was mounted approximately 4 mm from the sensitive surface of the diode, as shown in Figure 15.

The second modification was to the horizontal transverse stage. The micrometer drum was removed and a Precision Instrument, Inc. 48 tooth spur gear was mounted on the ground shaft. A mating 12 tooth gear was mounted to the output shaft of a gearhead synchronous motor with a 30.0 RPM output

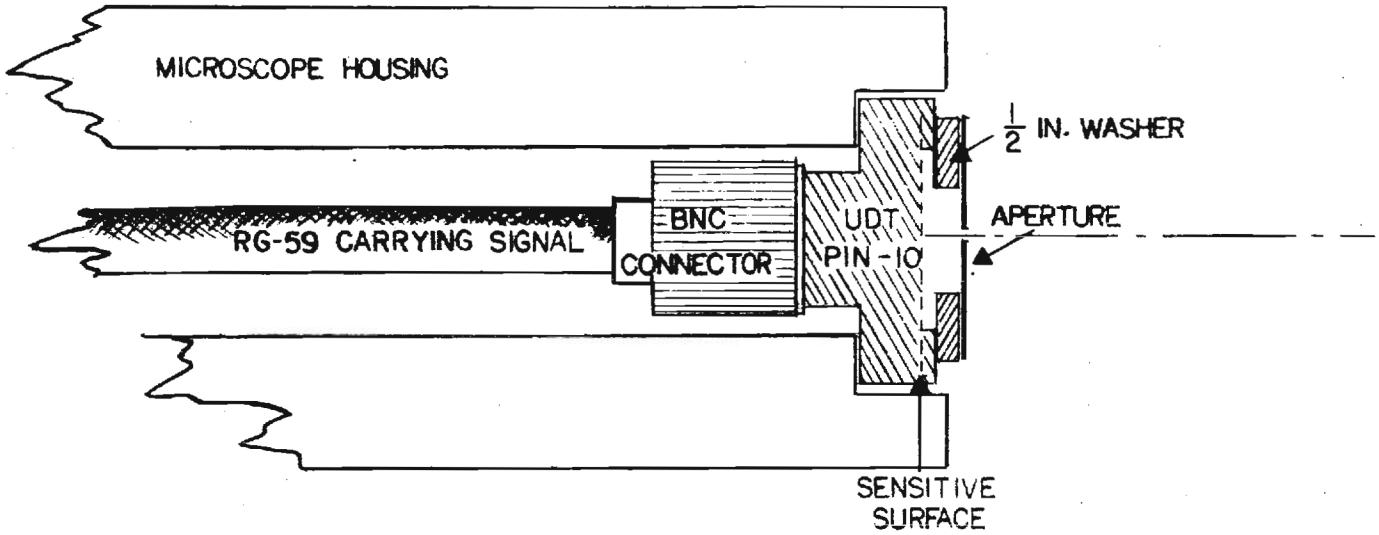

FIGURE 15. DETAIL OF BEAM PROFILE MEASURING DEVICE

shaft speed. As all measurements were conducted by a continuous scan, the gear backlash did not affect the measurements. The synchronous motor was mounted to the horizontal transverse stage. With the motor engaged, the slide travelled with a velocity of 1/40 in/sec x 30 rpm x 1/4 = 0.1875 in/min. or 4.7625 mm/min.

The signal from the photodiode was fed into a low pass filter that served to remove the small 60 Hz variation because of the room lights. The filtered signal was recorded with a Mosely Autograf Model 680 strip chart recorder.

Initial measurements indicated that the beam is not a centered Gaussian. In addition to being off-center, there were spikes present near the edge of the beam profile scan. The aperture assembly was adjusted to correct the centering problem. The aperture slides were almost 2 mm thick.

It was observed that the spikes were no longer present in the scan trace once the aperture slides had been reduced in thickness by use of a countersink. The scans recorded after these adjustments were made were observed to be very close to a Gaussian profile. Four consecutive scans were made with each of four apertures. Figures 16 and 17 illustrate the results for two of the apertures, 1.8 mm and 2.7 mm in diameter. The exact recorder traces for all four scans are superimposed and the outline of the ideal Gaussian profile is also given. In both cases the beam remains Gaussian over approximately 90 percent of the aperture and is truncated at the aperture edge.

B. Measurement of Scanner Access Time

The response of the scanner is limited only by the speed of the mechanical parts that move during the scanning process. The response of the scanner is, in effect, determined by the response of the galvanometer

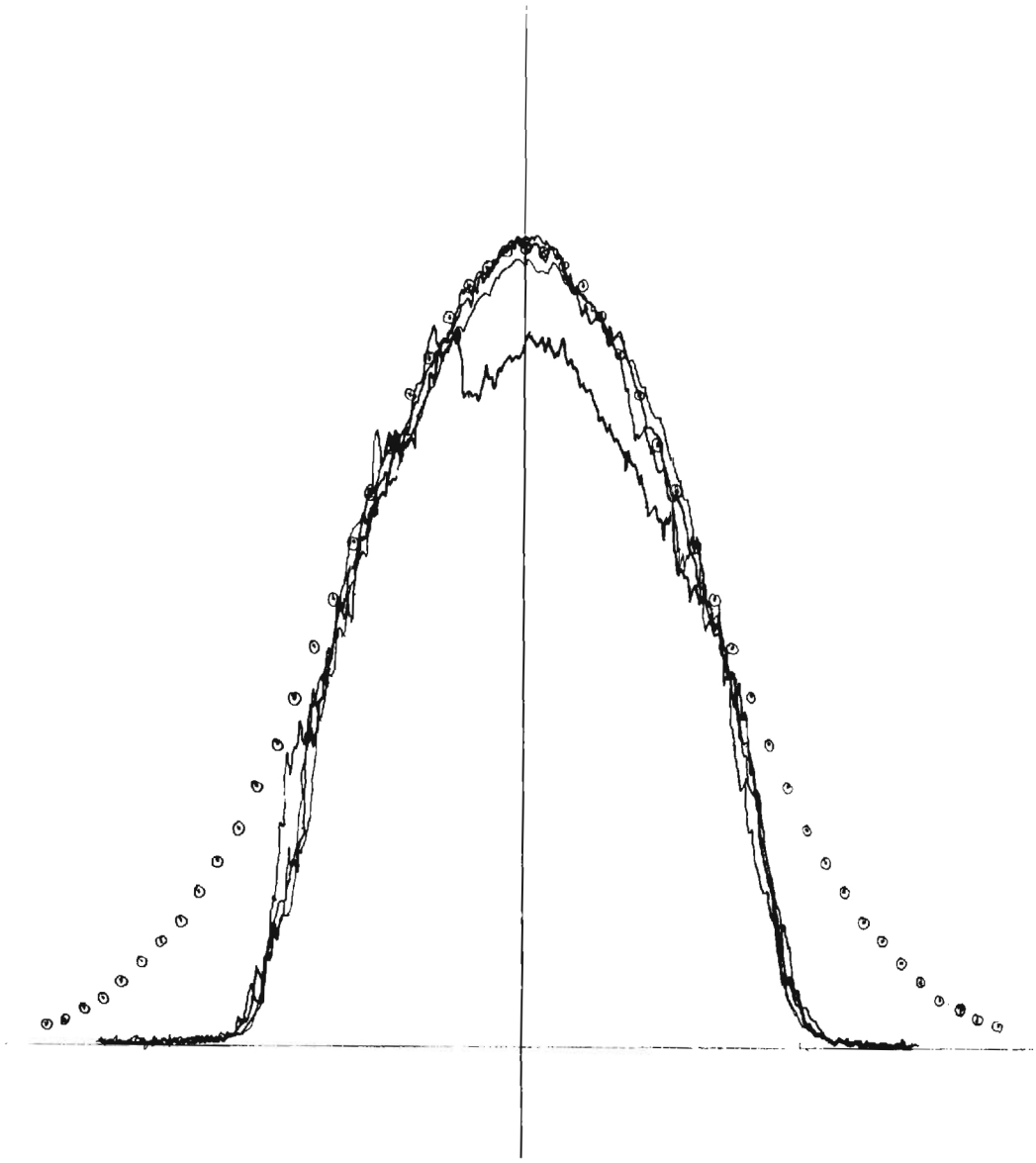

FIGURE 16. 1.8 mm DIAMETER APERTURE BEAM PROFILE

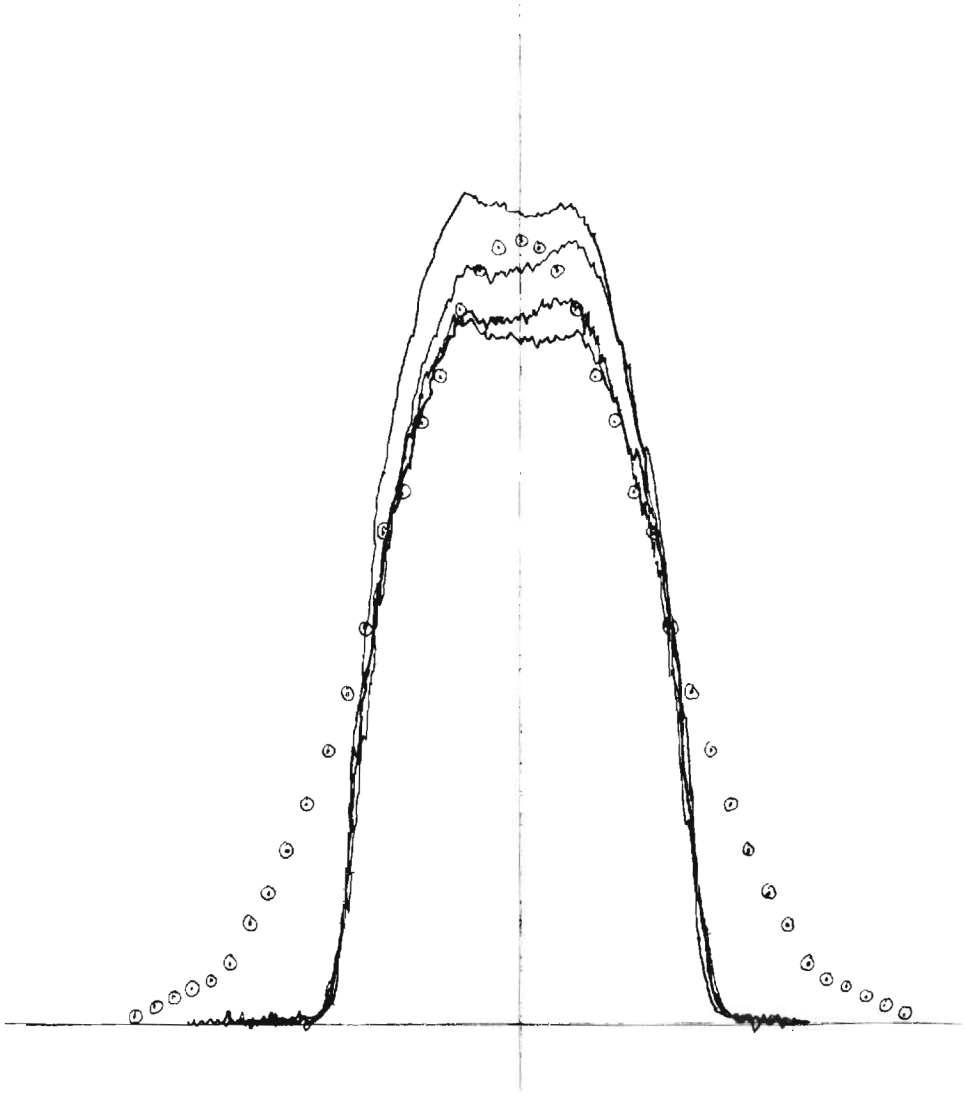

FIGURE 17. 2.7 mm DIAMETER APERTURE BEAM PROFILE

driven mirrors, as they are orders of magnitude slower than any other component in the scanner.

To measure the response time of the galvanometers, a step corresponding to approximately a 3° deflection was fed to the Model 108 PD galvanometer. The Model 108 PD contains a capacitance bridge that causes the resistance of the position detector circuit to vary in direct proportion to the mirror deflection. By displaying the response to a square wave and the square wave itself on a storage oscilloscope, and photographing the resulting traces, a permanent record of the response is obtained. The test apparatus is shown in Figure 18. This figure also illustrates the proper interfacing of the position detector circuit to the galvanometer.

Figure 19 is the resulting trace using a 2 Hz square wave. Both traces have a 2 msec/cm time base. From the figure, it is seen that the response time of the galvanometer is slightly greater than two milliseconds. The experiment was repeated several times with identical results.

C. Measurement of the Spatial Invariance of the Fourier Transform of the Scanning Beam

To further test the scanner's performance, two measurements were performed; the parallism of the scanning beam with respect to the optical axis, and the variation in spot size as a function of position (x, y address). Both of these measurements are important if the scanning beam is to be used to illuminate two dimensional images in an optical data processing system. The reason that these two factors are important is that both can affect the spatial (and temporal) invariance of the two dimensional Fourier transform. By directly measuring the Fourier transform as the beam scans, the effect of both factors can be observed.

To observe the Fourier transform plane, the experimental arrangement shown in Figure 20 was used. From the scanner, the beam was focused to a

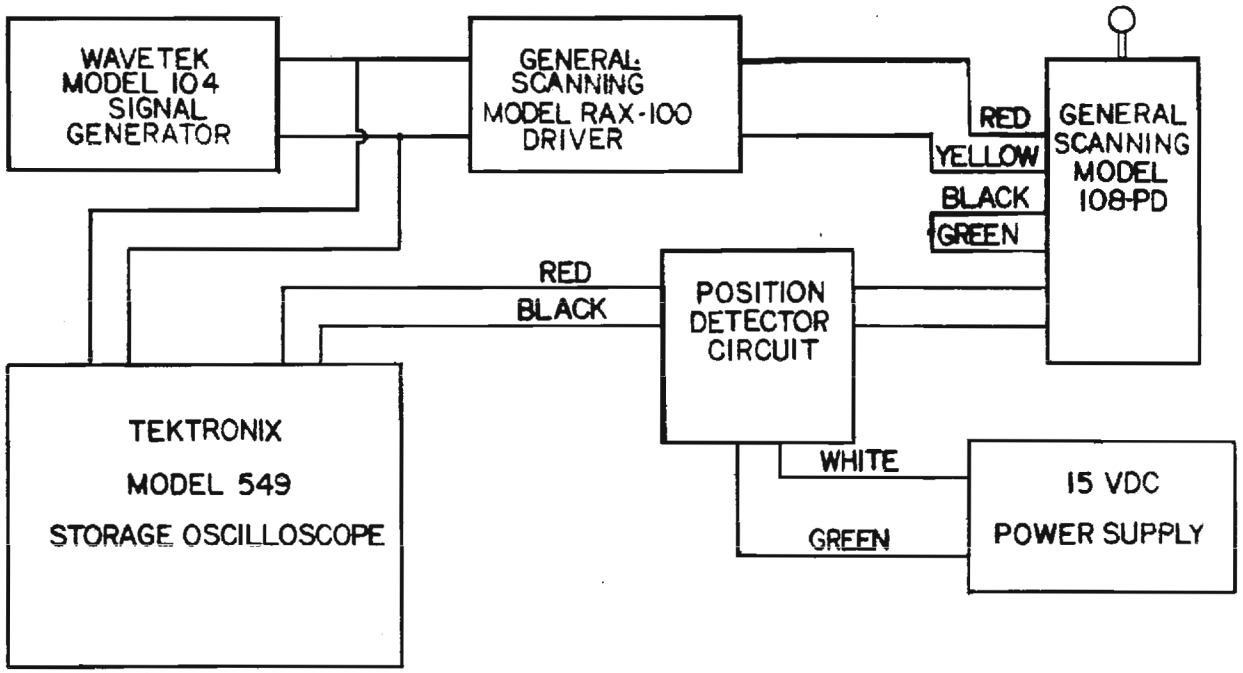

FIGURE 18. GALVANOMETER RESPONSE TIME TEST LAYOUT

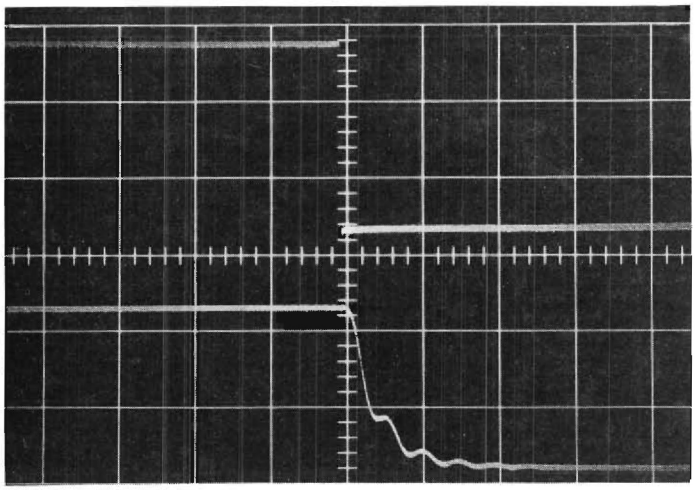

2 MILLISECONDS PER CENTIMETER TIME BASE

UPPER TRACE: INPUT
LOWER TRACE: RESPONSE

FIGURE 19. GALVANOMETER RESPONSE

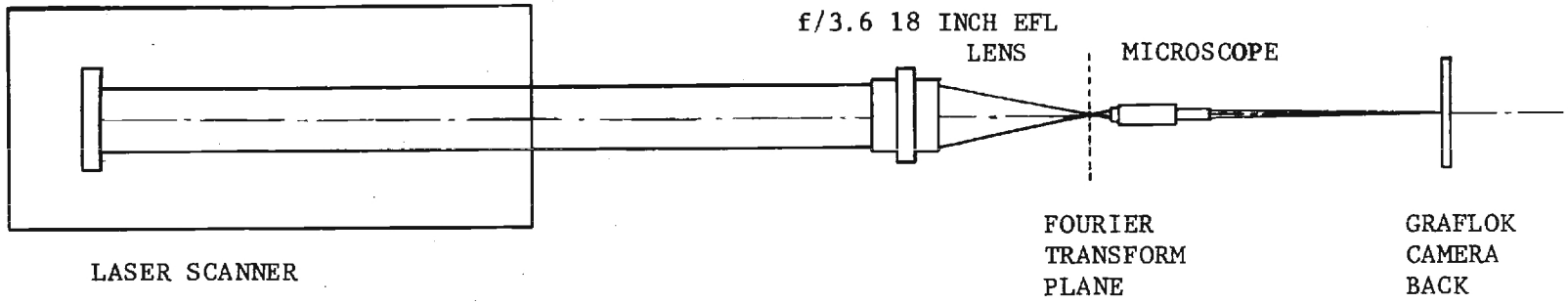

FIGURE 20. FOURIER TRANSFORM SPATIAL INVARIANCE TEST LAYOUT

two dimensional Fourier transform by a F/3.6, 45.72 cm focal length Cooke triplet. The Fourier transform was projected by a microscope using a 5x objective and 10x eyepiece, with a cross hair reticle, onto the ground glass of a mounted Graflok camera back. Because the lowest numerical aperture objective available (the 5x objective previously mentioned) was N.A. 0.12, the maximum acceptance angle of the microscope was limited to 13.8°. Using the 45.7 cm focal length transforming lens, the maximum measurable scanned format was limited to 5.48 x 5.48 cm (2.16 x 2.16 inches).

The y galvanometer was driven by a 28.5 Hz sine wave, and the x galvanometer was driven by a 700 Hz sine wave. The plates shown in Figure 21 are the photographs taken using the Graflok camera back. The exposures were approximately one second in duration. During this time the format was scanned at least 20 times. As the photographs of the transforms of the various apertures are very high contrast Airy discs, it is obvious that motion of the Fourier transform is very small. Visually, it was not observable using this apparatus.

To obtain an estimate of the sensitivity of the apparatus, we examine the transform photograph of the 2.7 mm aperture, Figure 21. From the Rayleigh criterion,

$$\theta = 1.22 \frac{\lambda}{D} \tag{22}$$

$$= 1.22 \frac{4.88 \times 10^{-7} m}{2.7 \times 10^{-3} m}$$

$$= 2.20 \times 10^{-4} \text{ radians.} \tag{23}$$

For a 45.72 cm focal length lens, the radius of the first dark ring is

$$\text{radius} = .4572 \times 2.20 \times 10^{-4} = 1.008 \times 10^{-4} \text{ m,} \tag{24}$$

or radius = 100 μm.

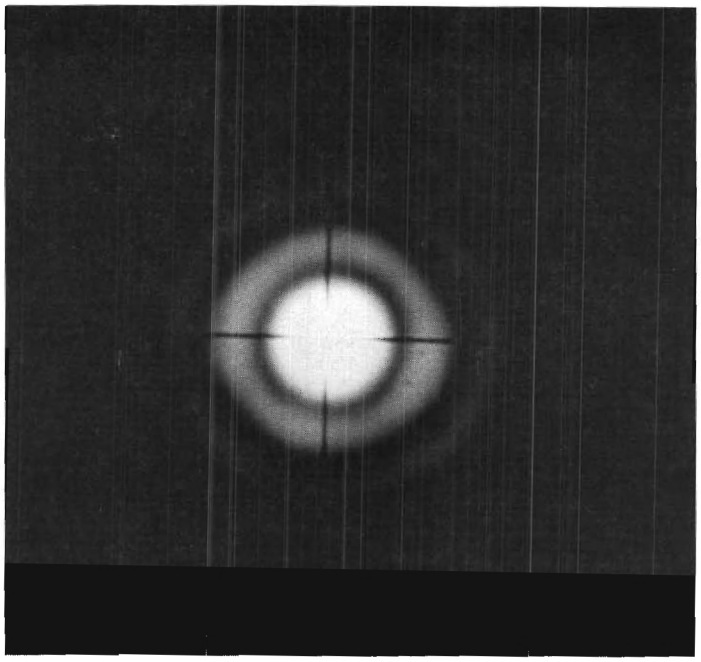

1.8 mm DIAMETER CIRCULAR APERTURE
63.5 DIAMETERS

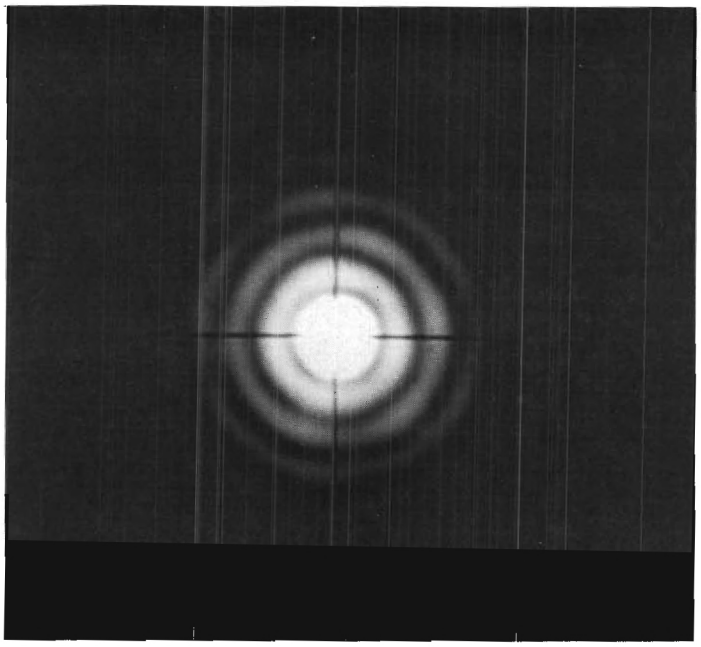

2.7 mm DIAMETER CIRCULAR APERTURE
63.5 DIAMETERS

FIGURE 21. PHOTOMICROGRAPHS OF FOURIER TRANSFORM PATTERNS

On the photograph, this corresponds to 6.35 mm, an enlargement of 63.5 diameters. The microscope focus was changed so that the image of the central ring filled the ground glass (ring radius = 45 mm). This resulted in a magnification of

$$\frac{4.5 \times 10^{4}\mu}{10^{2}\mu} = 450 \text{ diameters.}$$

Under this extreme magnification there was still no motion observed.

The human eye can resolve approximate 3×10^{-4} radians. Viewing the screen at a distance of 40 cm, one would be able to observe a motion of $0.4 \text{ m} \times 3 \times 10^{-4} = 120\ \mu\text{m}$. Therefore the transform is stable to less than

$$\frac{120 \times 10^{-6} \text{ m}}{450} \cong 2.6 \times 10^{-7} \text{ m} \cong \frac{\lambda}{2} \qquad (25)$$

A picture of the scanner during an operational test at Georgia Tech is shown in Figure 22.

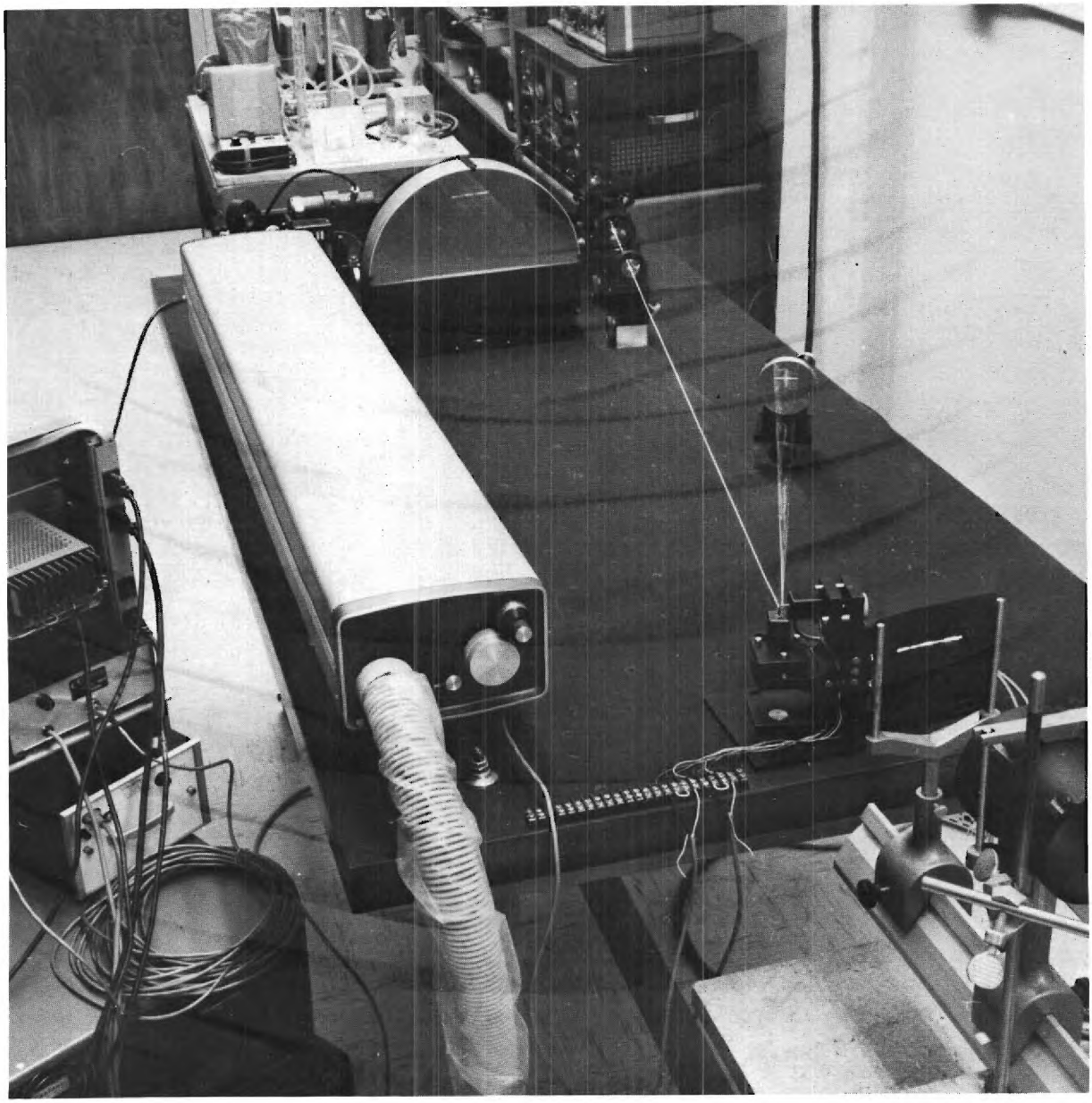

FIGURE 22. SCANNER DURING OPERATIONAL TEST AT GEORGIA TECH. SINGLE HORIZONTAL LINE IS BEING TRACED BY THE SCANNER ON THE AERIAL PHOTOGRAPH. (LOWER RIGHT HAND CORNER.)

V. ACKNOWLEDGEMENTS

We would like to express appreciation to Mr. Eric Griggs for his illustrations in this report. Mr. Bill Dittman provided excellent assistance in the mechanical design of the scanner. Discussion with Mr. L. D. Holland regarding the feedback control system is appreciated.

The cooperation of Mr. Joseph Kerr, Mr. Ellington Pitts, and Mr. H. Frayne Smith of NASA/MSFC and Mr. John York and Mr. Bill Evans of Sperry Rand Corporation was essential to the successful completion of the project.

APPENDIX A

Specifications for Genral Scanning Model 108 PD Galvanometer

Load Free (no mirror) Natural Frequency Hz	1,500
Mechanical Rotation	8°
Armature Inertia, gm cm^2	0.011
Torque Approx. Value gm cm	80
Coil Resistance, ohms (series)	8 $\pm$ 1,S
Sensitivity mA/degree	150
Linearity	1% of peak to peak, or better
Repeatability	0.05% of peak to peak, or better
Life, cycles	10^{11}
Weight, ounces	3